An analytical method for identifying synergies between behind-themeter battery and thermal energy storage

Matthew Brandt^{a,b}, Jason Woods^{a,*}, Paulo Cesar Tabares-Velasco^{a,b}

^aNational Renewable Energy Laboratory, 15013 Denver West Pkwy, Golden CO 80401, USA ^bColorado School of Mines, Golden CO 80401, USA

*Corresponding author: Tel: 1-303-384-6189; E-mail: jason.woods@nrel.gov

Abstract

Electric utilities build generation capacity to meet the highest demand period, and they often pass on the costs associated with these peaking generators to building owners through demand charges. Building owners can minimize these demand charges by shifting energy use away from peak periods with behind-the-meter storage. This storage can include batteries, which can directly shift the metered load, or thermal energy storage, which can shift thermal-driven electric loads like air conditioning. However, there is a lack of research on how best to combine battery and thermal energy storage. In this study, we develop an analytical sizing method to calculate the potential demand reduction and annualized cost savings for different combinations of thermal and battery energy storage sizes. We show that adding batteries to a thermal energy storage system can increase the total system's load shaving potential. This is particularly true when the building has onsite photovoltaic generation or electric vehicle charging, which add significant variability to the load shape. We also show that for a given total storage size, selecting a higher fraction of thermal energy storage can significantly lower the cycling of the battery, and therefore extend the battery life. This, combined with the expected lower first cost of thermal energy storage materials compared to batteries, shows that hybrid energy storage systems can outperform a standalone battery or standalone thermal storage system. Assuming the thermal storage has a capital cost 6x lower than the battery, our analysis shows that the optimal system is 71% thermal energy storage and 29% battery energy storage for a scenario with electric vehicle charging. The annualized cost savings for this system are \$48.6k/yr, whereas an equivalently sized standalone thermal energy storage system would provide annualized cost savings of \$28.5k/yr and a standalone battery would lead to savings of \$8.72k/yr. The hybrid system also reduces battery cycling by 52% compared to a standalone battery, extending battery lifetime.

1. Introduction

Buildings account for 75% of U.S. electricity consumption and 40% of total U.S. energy consumption [1]. Building cooling drives electric peak demand in summer and this is expected to become more challenging due to anticipated growth of onsite photovoltaics (PV) and electric vehicle (EV) charging. For example, Colorado has a goal to have almost 1 million EVs by 2030 [2] and California plans to have 250,000 EV charging stations by 2025 [3]. The increased load from these EV chargers, along with increased renewable energy capacity, will drive the need for flexible resources to balance supply and demand on the electric grid.

Energy storage is expected to play a significant role in mitigating high electric demand charges, including behind-the-meter storage, in which assets used for energy shifting and demand management are owned and controlled by the customer. Behind-the-meter storage can include electrochemical battery energy storage (BES) and thermal energy storage (TES); however, there are no standard methods to guide the process of selecting, sizing, or controlling these two assets together to maximize energy cost savings. While many studies have developed approaches for optimizing a single storage type, relatively few have considered the tradeoffs and benefits from using a hybrid battery/TES system.

Battery costs are declining, but batteries still tend to be more expensive than a comparable TES system due to higher capital expense, faster life-cycle degradation, and potentially higher operation costs [4]–[7]. Batteries are considered more flexible since they directly meet the electrical load for which the consumer is billed [8]. In contrast, TES uses less expensive materials than batteries and has the potential to have a lower first cost [9], but can only be used to address thermal loads. Since cooling drives peak demand on the grid and typically coincides with the highest electricity rates, cold TES can still make significant contributions to peak management. These differences between batteries and TES make any direct comparison or operating decision challenging.

Battery control and sizing have been the subject of substantial research, both in terms of grid- and customer-side load management using both optimization and rule-based approaches as summarized in numerous review papers (e.g., [10]–[13]). In behind-the-meter TES, research has focused on smart controls, new materials development, systems integration, and performance for both cooling and heating applications ([14]–[18]). These systems can use sensible storage capacity in water tanks or concrete, and solid-liquid phase change materials (PCMs). There are many review articles summarizing the state of the art of TES for cooling applications (e.g., [14], [16], [19]–[21]).

A few researchers have considered combinations of batteries and thermal energy storage and relied on optimization algorithms that tend to require large computational resources. For example, Hu et al. paired a battery with ice storage for a district cooling system in Singapore and used mixedinteger linear programming (MILP) and model-predictive control to size and control the hybrid system [22]. Niu et al. investigated the use of batteries with flexible air conditioners by using building thermal mass. Their MILP model used a forecast of the cooling demand to minimize operating costs under a time-of-use rate structure [23]. Meinrenken and Mehmani found that combining batteries with controllable air conditioners by using building thermal mass reduces peak demand for a multi-zone office building in New York by 26% and electricity costs by 11% [24]. Vedullapalli et al. optimized the heating and cooling setpoints and battery controls to minimize electricity costs for a small office in Charleston, SC using MILP and model predictive control [25]. Wang et al. numerically combined a battery with a chiller and cold-water tank, showing the effects of downsizing the systems and improving efficiency [26]. Hu et al. analyzed an office building and showed that adding a chilled water storage tank for air conditioning reduces the required battery capacity by 85% [5]. They used the battery for frequency regulation and the thermal storage as a contingency reserve for the grid. Borland et al. showed that an experimental residential home in Hawaii could reduce the grid-purchased electricity by 94% by adding PV, battery, and thermal storage [27].

This previous research shows the potential for hybrid energy storage systems compared to a single-type storage system. However, there are several limitations. Most studies focused on a particular installation and did not explore different combinations of thermal and battery energy storage sizes. Many studies simply added a thermal storage and determined how much smaller

the battery could be. Cases considering building thermal mass only analyzed one TES size, as the size is fixed by the mass of the building materials. Some studies consider onsite PV, but none consider how the significant increase in EV charging at buildings will impact the tradeoff between battery and TES.

Optimization results can be difficult to generalize, and the influence of different factors must be analyzed on a case-by-case basis. Furthermore, the majority of these software tools use MILP, so physical phenomena must be linearized, which could impact the fidelity of results. By comparison, analytical techniques can obtain similar solutions with lower programming and computational overhead. Analytical techniques can complement optimizations by addressing some of the potential drawbacks described above, especially in directly relating inputs and outputs in concise formulations and capturing nonlinear phenomena by integrating high-fidelity physics-based models that do not need to be linearized. For example, Wu et al. demonstrate a promising analytical approach to sizing batteries and obtain a solution within 1% of the optimization-based result [28]. Their approach analyzes the peak day and compares the incremental utility cost savings with the incremental capital costs to find the maximum useful battery size. Thus, the authors directly relate the pseudo-optimal power and energy capacities to the load profiles, utility rate structures, and capital costs. However, the author's approach is only applied for a standalone battery.

In this study, we propose a simple method for sizing a hybrid battery/TES. We compare the annualized cost savings of hybrid storage systems with systems that include only a battery or only a TES. The novel contributions of this paper are: (1) a new analytical and flexible technique for sizing and identifying the idealized dispatch for hybrid and standalone storage systems, which does not depend on complex optimization algorithms, (2) analytical evaluation of the performance of hybrid energy storage systems, compared to a battery alone or TES alone to illustrate the tradeoffs and synergies of battery and TES, and (3) analysis on how onsite PV generation and extreme-fast EV charging influence the load profile shape (i.e., the load duration curve) and the sizing of hybrid energy storage systems.

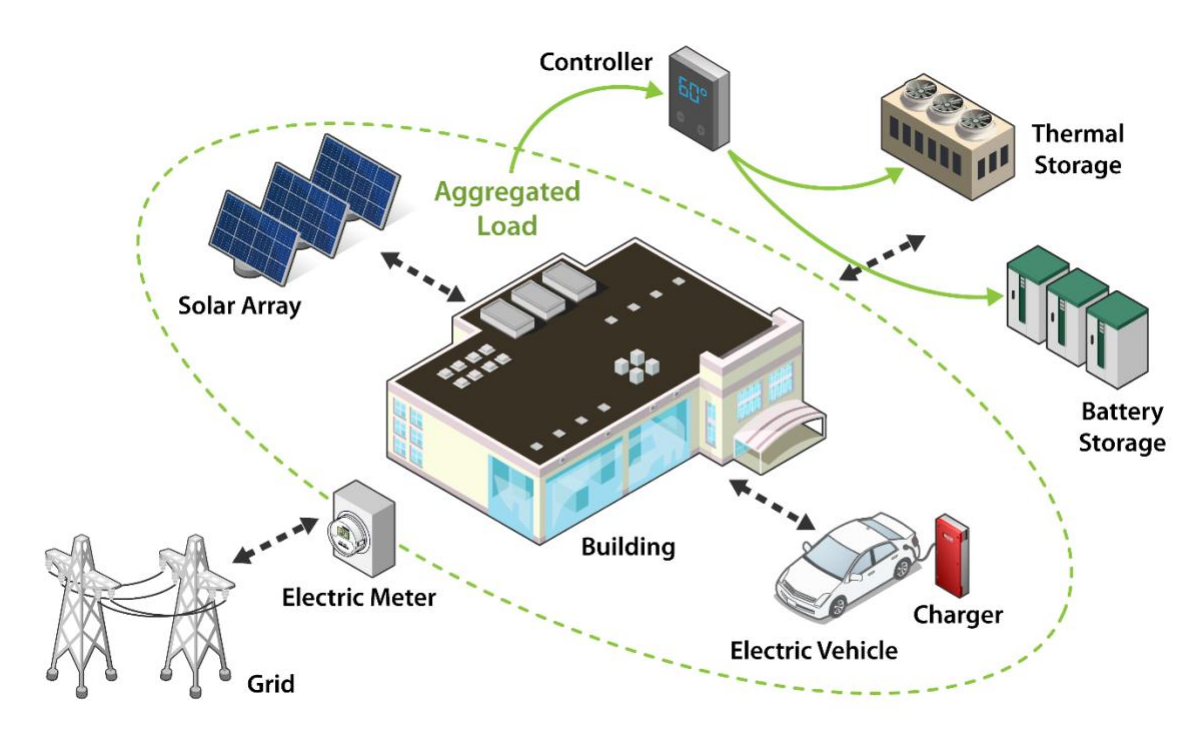


Figure 1: Reprensentation of the the analytical sizing method presented in this study, demonstrated with a simulated big-box grocery store, EV charging, PV generation, and behind-the-meter battery and thermal energy storage

2. Methods

This section introduces the new analytical method for sizing hybrid energy storage systems for demand reduction. The method is demonstrated using scenarios based around a simulated big-box grocery store with EV charging stations and PV (Figure 1), and this study focuses on behind-themeter battery and thermal energy storage systems with an idealized dispatch based on the aggregated baseline load. Figure 2 shows a flow chart of the overall approach, which is a visual outline of this paper's methods and results. The approach requires three primary inputs: (Section 2.1) the variable utility rate structure, (Section 2.2) the energy storage system(s) to be analyzed, including efficiency and performance characteristics, and (Section 2.3) electric demand power profiles at the meter for both the total and thermal loads. In this study, the method is demonstrated using simulated data, so Section 2.3 describes the models used to create the electric load profiles for the big-box building, EV charging stations, and PV generation.

Section 2.4 presents the idealized dispatch algorithm, which determines the maximum possible peak demand reduction and/or energy shifting for a range of battery and thermal energy storage sizes for a complete year. Results from the algorithms are post-processed to analyze other

outcomes, such as annual utility cost savings, battery cycling, or total cost savings (Section 2.5). Finally, Section 2.6 describes a sensitivity analysis to determine how the overall trends and conclusions depend on the assumptions.

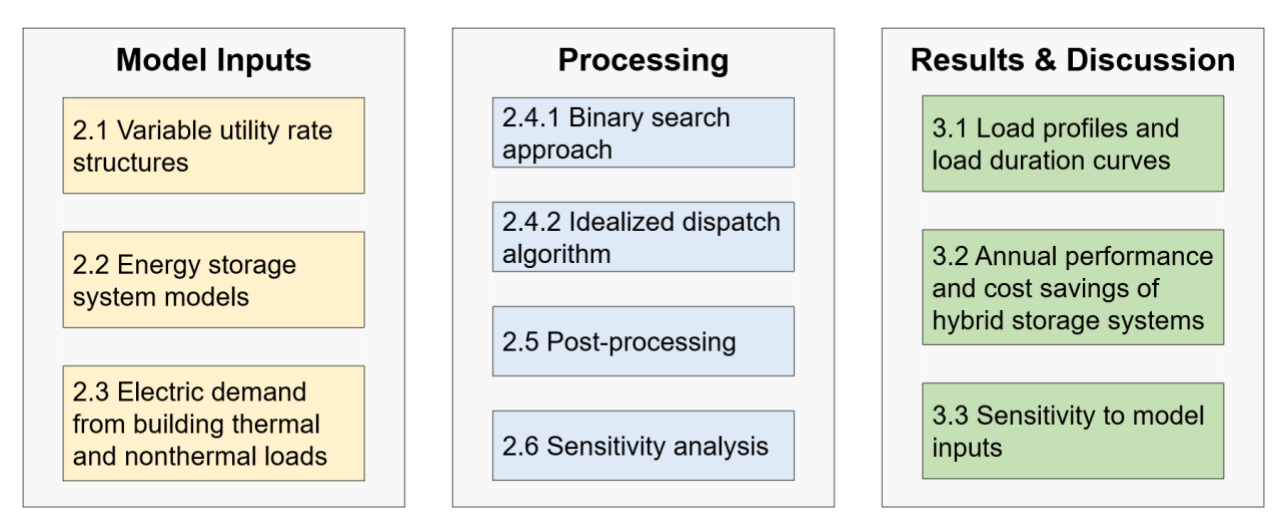


Figure 2: A visual outline for this study which shows the Inputs, Processing, and Results used to explain and demonstrate the proposed analytical sizing and dispatch approach for hybrid energy storage systems

2.1 Variable utility rate structures

Variable electric rates are needed to incentivize energy storage and thus are an important input for this method. Commercial utility electric rate structures often have peak-demand charges or time-of-use rates. Such rate structures encourage users to charge energy storage systems in less expensive periods and discharge the stored energy during more expensive periods. Demand charges commonly range from 10-30 \$/kW, though they can be as high as 90 \$/kW for commercial and industrial consumers [29]. They are assessed using the maximum demand power, typically in the trailing 15-minute moving average of the metered load for some period in a billing cycle (typically all time, an on-peak period during a monthly billing cycle, or a combination of both).

Although this approach can also be used with time-of-use electricity rates, this study focuses on the peak demand reduction potential of hybrid battery/thermal energy storage systems. The utility rate structure includes a flat energy price of 0.12 \$/kWh and a demand charge assessed for all time in a monthly billing cycle of 15 \$/kW. The study also explores the impact of assessing demand charges on all months or only for the cooling season (May to September).

2.2 Energy storage system models

The proposed methodology uses simple storage models that do not represent specific energy storage systems but capture the overall trends, tradeoffs, and potential synergies of a hybrid battery/thermal energy storage system [30]. For example, the battery is not based on a particular chemistry, and the thermal energy storage model is not based on a particular brand, set of components (e.g., chiller, ice tank), or storage media (e.g., ice). The battery and thermal energy storage models are defined by a constant electrical round-trip efficiency and specified maximum allowed rate of discharge (as a C-rate). Note that a charging power constraint is not imposed on either system because there are typically more timesteps available to charge the storage than are used for discharge (e.g., an 8-hour on-peak period will have at least 16 hours of off-peak time available for charging). Therefore, the charge power remains low, at least for the scenarios considered in this study. The state of charge is also constrained between 0 and 100%, based on the nominal energy capacity. In this study, we do not model any changes in the SOC limits due to changing ambient conditions or required discharge power. For example, the capacity of most batteries is lower than nominal at low temperatures, and TES capacity drops below nominal at high discharge powers since the outlet temperature exceeds the cutoff temperature [31]. We also do not consider any impact of the history of state of charge levels on lifetime.

2.2.1 Round-trip efficiencies for analyzed storage systems

Equation (1) defines the energy storage electrical round-trip efficiency (η_{ES}) as the ratio between metered electrical energy avoided by the storage system's discharge and the electrical energy supplied to the storage system during charging. The "avoided" energy, $E_{avoided}$, is the consumed energy that would have otherwise been met by the grid had the owner not discharged energy from the storage system. The "supplied" energy, $E_{supplied}$, is the electrical energy used during off-peak periods to charge the storage. This term captures, for example, the electrical energy to the battery or electrical energy to the chillers which freeze an ice tank.

$$\eta_{\rm ES} = \frac{E_{\rm avoided}}{E_{\rm Supplied}} \tag{1}$$

The round-trip efficiency defined in Equation (1) is equivalent to the battery's round-trip efficiency—the ratio between the electric energy available for discharge and the energy required to charge the battery.

To compare with the battery round-trip efficiency, an equivalent electrical round-trip efficiency, η_{TES} , is defined for thermal energy storage systems in Equation (2). The avoided electrical energy is the difference between the electrical energy which would have been needed to meet the thermal load with baseline equipment, E_{base} , and the electrical energy required to discharge the TES, $E_{discharge}$ (e.g., from pump energy associated with increased pressure drop in the thermal storage system).

$$\eta_{\rm TES} = \frac{E_{\rm base} - E_{\rm discharge}}{E_{\rm charge}} \tag{2}$$

In Equation (3), each term is substituted with its corresponding thermal energy and average coefficient of performance (COP). The COP is the ratio of thermal energy output, Q, to electrical energy input, E, and therefore E = Q/COP. The electrical energy needed to discharge the TES is typically very small compared with $E_{\rm base}$. Thus, Equation (2) becomes:

$$\eta_{\text{TES}} = \frac{\frac{Q_{\text{base}}}{COP_{\text{base}}}}{\frac{Q_{\text{charge}}}{COP_{\text{charge}}}}$$
(3)

Neglecting losses in transmission, the thermal energy delivered to the zone, $Q_{\rm base}$, is equal to the thermal energy discharged from the storage, $Q_{\rm discharge}$. Substituting the ratio of thermal energy terms as a thermal round-trip efficiency, $\eta_{\rm TES,th} = Q_{\rm discharge}/Q_{\rm charge}$, yields Equation (4), which relates terms typically associated with characterizing a thermal energy storage system (i.e., COP of charging, COP of baseline equipment, thermal losses) in a form that is equivalent to the electrical round-trip efficiency of a battery. Thus, the two systems may be quickly compared for electrical energy shifting efficiency.

$$\eta_{\rm TES} = \left(\frac{\overline{COP_{\rm charge}}}{\overline{COP_{\rm base}}}\right) \eta_{\rm TES,th}$$
(4)

Batteries' round-trip efficiencies are typically specified by the manufacturer and are commonly between 85-95% [6]. Thermal storage systems have a higher range of possible values, varying between 80-115%, because the expression depends on more variables, including condenser-side (ambient) and evaporator-side (zone) temperature dependence of COPs for charging and discharging, as well as thermal loss variables [32]. The "efficiency" being higher than 100% is technically possible due to the differences between the charging COP and the baseline COP. For

example, if the ambient temperature during charging is lower than the ambient temperature during discharging, then the temperature lift during charging is lower, and the ratio of COP_{charge} to COP_{base} may be greater than 1. In this analysis, we focus on other aspects of these storage systems, and thus we assume constant electrical round-trip efficiencies of 90% for both energy storage systems.

2.2.2 Discharge energy capacity and maximum C-rates for analyzed storage systems

The discharge C-rate is the ratio of discharge power to the nominal discharge energy capacity. For example, a discharge rate of 1C will deplete the storage in 1 hour, while 2C depletes the storage system in 0.5 hours. Thus, in this study, the discharge power capacity is calculated as the discharge energy capacity divided by the maximum C-rate.

In any simulation, the highest possible discharge rate is the discharge power that results in the system being fully depleted in one timestep, since discharge must be uniform during the entire timestep. Therefore, 4C is the maximum possible discharge C-rate for simulations presented in this study, which use 15-minute timesteps. Additional constraints to the discharge rate may be imposed for either system in this model. Here, the battery discharge is limited to 1C while the TES remains free to discharge at up to 4C. Although 4C may seem unrealistic for thermal energy storage, the approach documented in this study prioritizes thermal storage over battery storage. With such prioritizing, high C-rates are only seen for storage systems with relatively small TES sizes. The sensitivity to these assumptions is explored in the sensitivity analysis described below.

2.3 Electric demand power profile and load duration curves

In this study, we analyze simulated electric demand power profiles for different scenarios combining a building with EV charging stations and/or PV generation. The following sections describe how the building total and thermal load, PV generation, and EV load profiles are obtained.

• <u>Building</u>: This study uses an EnergyPlus model for a big-box store with both grocery and retail zones, which was calibrated to data from a store in Centennial, CO [33]. This calibrated model is simulated using EnergyPlus Version 9.3.0 and typical meteorological year (TMY3) data for the Sky Harbor International Airport in Phoenix, AZ. Phoenix was selected due to its high average temperatures and long cooling season, which translates to higher potential for TES utilization. However, the proposed methodology could apply to other building types and climate zones. The annual load profile is shown in Figure 3. Note

the nonzero thermal load in winter, and the strong dependence of the total load on the thermal cooling load.

- **EV charging model**: The EV charging profiles simulated in this study presume a relatively aggressive transition to EVs nationwide. The EV profile was generated using EV-EnSite, which is a direct current fast charging (DCFC) model based on EVI-Pro. We followed the methods from previous research [33]–[36]. This study uses a 350-kW charging rate and 6 charging stations on the same meter as the building. Each station has 16 events per day. The events are 5-15 minutes long depending on the state of charge of each vehicle's battery when it arrives at the charging station.
- **PV generation**: PV generation profiles are simulated using the "Detailed PV Model" in NREL's System Advisory Model (SAM), Version 2020.2.29 Rev. 2 and the same weather data as the building model. The resulting generation profile is scaled so that the peak power provided by the PV array is 600 kW. Cubic spline interpolation is applied to increase the resolution from 1-hour timesteps to 15-minute timesteps.

These three sub-models are used to create four scenarios, listed below. The total electric demand power profiles for the entire year and for a peak day for each scenario are shown in Figure 3.

Scenario 1) B: Baseline building with no PV and no EV charging

Scenario 2) B+PV: Building with 600 kW of rooftop PV and no EV charging

Scenario 3) B+EV: Building with no PV and 6 EV charging stations

Scenario 4) B+PV+EV: Building with 600 kW of rooftop PV and 6 EV charging stations

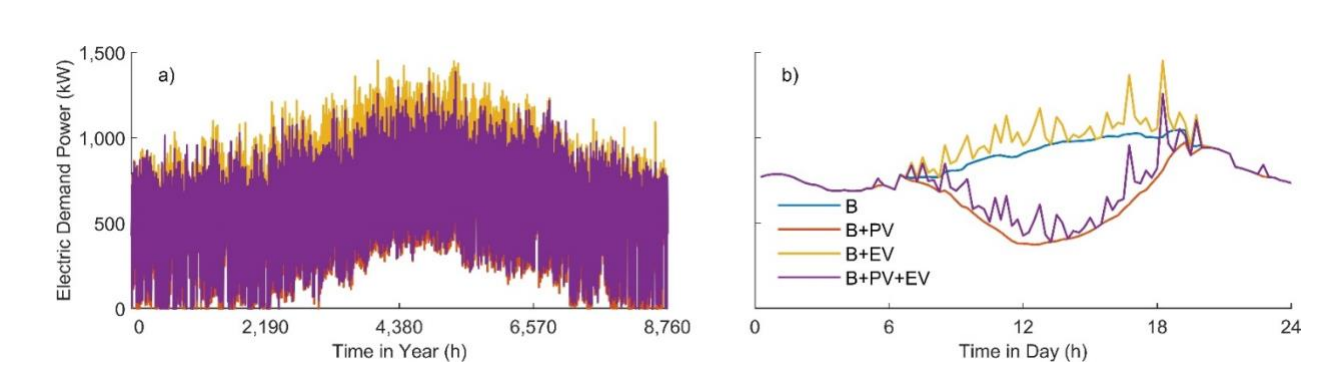


Figure 3: Simulated total electric demand power profiles for the four scenarios for (a) the entire year and (b) the summer day with the highest peak demand for any scenario (B+EV scenario) using a 15-minute timestep

Figure 3 shows the electric load profile for the entire year (Figure 3(a)) and for a summer day (Figure 3(b)) for each scenario: building (B, blue line), building with 600 kW of rooftop PV (B+PV, red line), building with 6 EV extreme fast charging stations (B+EV, yellow line) and building with both the PV and EV charging (B+PV+EV, purple line).

On June 19, the B+EV scenario has the highest peak demand of any day, as shown in Figure 3(b). The baseline building peaks in the evening due to increased air conditioning loads in the hot part of the day. EVs introduce significant variability to the load profile, increasing demand by up to 500 kW over 15- to 30-minute durations. Rooftop PV reduces the building profile during daytime, lowering the day's peak by 7% and shifting it to later in the day. This also increases the ramp rate to ~175 kW/hr for the evening hours as the PV production declines and electric demand remains high. Including both EV and PV shows how significantly varied the load can be when metered-load reducing assets (e.g., PV) are combined with metered-load increasing assets (e.g., EV).

These profiles can also be visualized using load duration curves, which are obtained by sorting the electric load profile in descending order. We then overlay the coincident thermal load (i.e., the thermal load is sorted in the same order as the total load). For example, Figure 4(a) shows a monthly total and thermal electric load profile for the baseline building, and plot (b) shows the corresponding load duration curve. The battery can operate on any electric load (blue) while TES can only shift electric loads associated with a thermal load (red). The maximum demand power of nonthermal loads (highest point on yellow curve) represents the lowest value to which an idealized TES can shave the total peak demand for a given month, since TES cannot be used to deliver electricity for nonthermal loads. These profiles show the potential applicability of batteries and thermal storage, and how they can be used together to reduce peak demand.

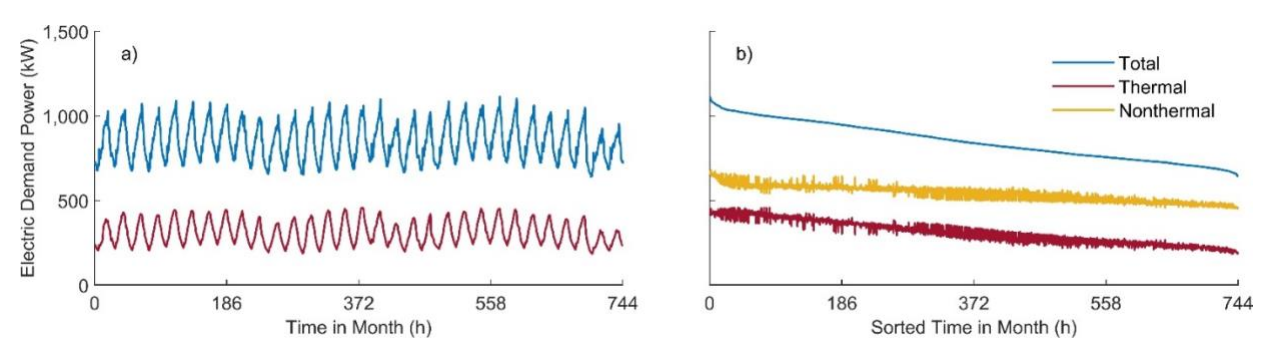


Figure 4: Constructing a load duration curve; (a) shows the time-ordered total (blue) and thermal (red) load profiles for one month; (b) shows the load duration curve (blue), and the coincident thermal (red) and nonthermal (yellow) loads for the month

2.4 Idealized dispatch algorithm

In this study, a range of hybrid systems are parametrically analyzed. Once the range of systems to be analyzed is determined (see Appendix A), the idealized dispatch required to maximize the peak demand reduction potential for a given system is calculated. This algorithm uses a binary search approach, described below in Section 2.4.1. The application of the binary search approach in the idealized dispatch algorithm is discussed in Section 2.4.2.

2.4.1 Binary search approach

The core of the dispatch algorithm is based on a binary search, in which a solution is known to exist between an upper and lower bound. The solver will update guesses, reducing the range of the bounds by half each time, until the solution is obtained (or the change on each iteration is sufficiently small). In this problem, the "solution" is the value of peak electric demand after shaving has reduced peak demand as much as possible (or as much as profitable, if the utility rate structures are not sufficient to justify peak shaving or energy shifting, see [28]). Meanwhile the initial bounds depend on the utility rate structure. For the utility rate structures considered here (demand charges assessed at all times in the billing cycle), the minimum peak demand occurs when the load is flattened; thus, the initial bounds are set to the maximum and minimum total load.

The binary search for the minimized peak demand power is illustrated in Figure 5. Frames 1-4 show how the storage-shifted load profile is calculated for a given guess. The solid blue stair profile is a total electric power profile for some arbitrary building. The solid black line represents the current guess. Starting with the first timestep in which discharge of stored energy is required

(i.e., the load exceeds the guess), the solver identifies the energy and power required to shave the load to the guess and increases the load to charge storage during off-peak times in the preceding 24 hours (Frame 2). The light-red area is the energy avoided by utilizing TES, while the light-yellow area shows the energy avoided by utilizing battery storage. The current algorithm uses a valley filling approach for charging, though this could be improved/changed depending on the objective. For example, charging could prioritize timesteps with the most favorable COP or seek to charge the storage as uniformly as possible (i.e., constant electric power supplied to storage). In these algorithms, TES is prioritized, but it is still inherently limited by the presence of a thermal load. Frame 3 shows the process continuing while Frame 4 shows the final discharge timestep being accounted for. After accounting for all required charging needed to discharge the storage system during discharge timesteps for the presumed guess, Frame 4 shows the resulting storage-shifted load profile in a dashed blue line (and Frame 5 shows the same case, but without highlighting the final discharging timestep with unique colors).

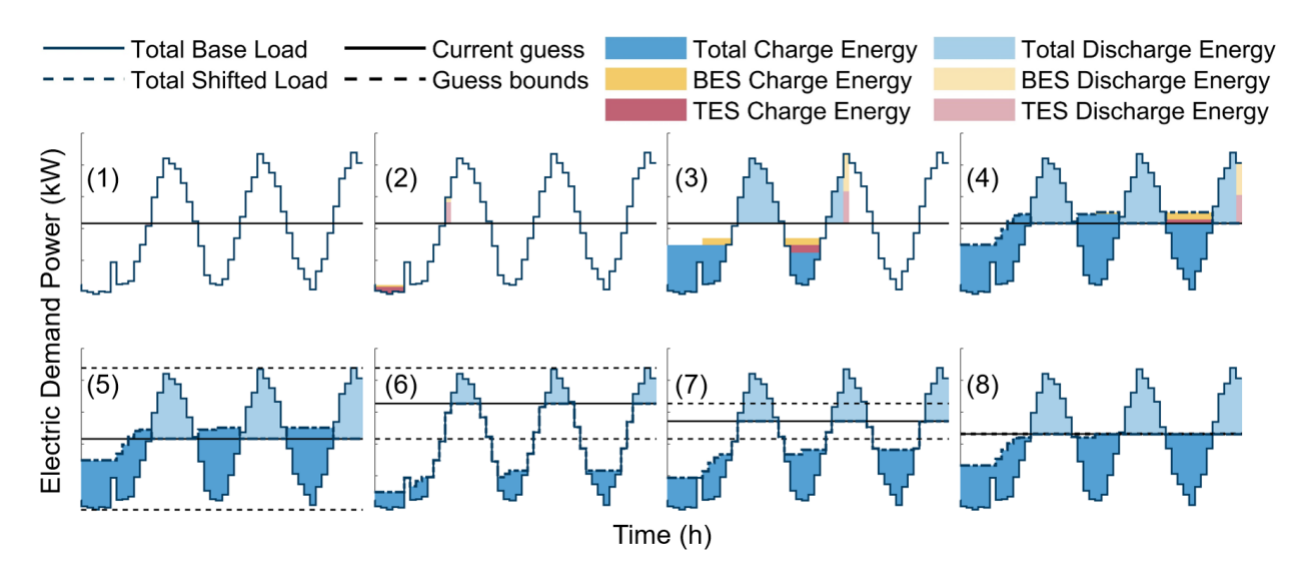


Figure 5: Visual representation of discharging/charging strategy for a given guess (Frames 1-4) and updating guess in binary search (Frames 5-8)

In the case of the guess value used in Frames 1-4, the shifted load profile exceeds the guess value. Thus, the specified storage system(s) are unable to shave the load to the guess value, and the presumed amount of shaving should be decreased. Frame 6 shows the updated guess in which less shaving occurs, halfway between the upper bound and the previous guess. In Frame 6, the shifted load never reaches the guess value, indicating that more shaving is possible. Therefore, in Frame 7,

the guessed amount of shaving is increased. This continues until the solution is obtained to within the desired tolerance, as shown in Frame 8.

2.4.2 Idealized dispatch algorithm for different combinations of BES and TES

The idealized dispatch algorithm is based on this binary search approach. For each month of the year, the maximum possible demand reduction that can be obtained with some hybrid storage system is calculated by applying the binary search algorithm, subject to the system's power and energy capacities. The dispatch algorithm uses the following steps.

- A. <u>Determine the range of battery and TES capacities to analyze</u>: In theory, any size of energy storage system could be defined and analyzed with this algorithm. To specify an upper bound, the sizing algorithm discussed in Appendix A is repeated for each month in the year. The month with the maximum useful battery is used to set the upper bound of systems analyzed, to avoid analyzing clearly oversized systems.
- B. <u>System selection</u>: A nested for loop cycles through every combination of energy and power capacities for both components in the hybrid system to be analyzed. Step C is repeated for each combination.
- C. Determine the peak demand reduction for each month in the year, for the given storage system: The maximum possible peak demand reduction is calculated for each month with a demand charge for the given storage system. The demand reduction is calculated using the binary search method described in the previous section, where the guessed amount of peak shaving is increased, subject to the requirement that none of the required power and energy capacities exceed the specified system's capacities. TES discharge is always prioritized since it must shift a thermal load, while BES can shift any load.

2.5 Post-processing

After calculating the potential peak reduction for each month, the algorithm output is processed to obtain demand charge/utility cost savings, annual equivalent full cycles of the battery, and annualized cost savings (accounting for annualized capital costs of the storage system). These metrics taken together are used to identify tradeoffs and synergies of hybrid storage systems.

2.5.1 Utility cost savings

The total utility bill the customer pays is comprised of demand charges and energy costs. The portion of the utility costs associated with demand charges (in \$/kW) is reduced by dispatching the storage system to lower the metered peak demand. However, the contribution to the total bill associated with the energy costs (in \$/kWh) increases due to energy losses, since the round-trip efficiency of both components is less than 100%. The annual utility cost savings, *UCS*, may be expressed as:

$$UCS = \left(\sum_{m=1}^{12} PS_m\right) p_{\rm D} - E_{\rm discharge} \left(\frac{1}{\eta_{\rm HES}} - 1\right) p_{\rm E} \tag{5}$$

where PS_m is the peak shaved in month m, p_D is the demand charge in \$/kW, $E_{\rm discharge}$ is the total energy of discharge over the year for the battery and thermal energy storage system in kWhe, and p_E is the flat energy rate in \$/kWh. When the demand charges are only assessed for summer months, PS_m is 0 kW for months without a demand charge. The storage system will be dormant since, at least for the example used here, there is not a sufficient opportunity for utility cost savings using energy storage if the energy rates are flat and no demand charge is imposed. The hybrid round-trip efficiency, $\eta_{\rm HES}$, is the discharge energy weighted average of the two components' efficiencies.

2.5.2 State of charge profile and annual battery cycling

After calculating the timesteps for discharge and charge in the final solution, the state of charge (SOC) for each component of the hybrid system is constructed. In this study, the battery cycling is simply characterized by the annual equivalent full cycles (EFC) method, which sums all discharge over the year, $E_{\text{BES,discharge}}$, and divides by the nominal capacity. For example, four consecutive cycles of 25% depth-of-discharge is one equivalent full cycle.

2.5.3 Annualized cost savings

The annualized cost savings are calculated by subtracting annualized energy storage capital costs from the annual utility cost savings ([28], [37]). We define the storage systems' annualized capital costs in terms of a constant lifetime and a fixed capital cost per unit of electric-equivalent discharge energy capacity (\$/kWh_e).

2.6 Model inputs and sensitivity analysis

Table 1 shows the nominal parameters used for the simulations below. The battery cost in \$/kWhe includes all balance of plant and installation costs for a 1-hour duration (i.e., 1C) battery [38]. The TES cost in Table 1 is \$100/kWhe, based on the typical \$/kWhth cost of existing chiller with ice storage projects (including installation costs), scaled by a presumed COP of 3.14 to convert this to \$/kWhe [37]. We also look at a special case where the TES capital cost equals the BES capital cost (\$600/kWhe), which shows the tradeoffs between the two storage systems when capital cost is not a factor. In addition to the nominal parameters shown here, we conduct a sensitivity analysis to determine how the results and conclusions are influenced by our assumptions.

Table 1: Analyzed parameters (Nominal) and variations explored (Low-High)

Parameter	Low	Nominal	High
BES C-rate Limit (1/h)	0.5	1	2
BES Capital Cost (\$/kWh)	300	600	900
BES Lifetime (yr)	10	15	20
Demand Charge (\$/kW) ^a	7.5	15	22.5
Discount Rate (%)	4	8	12
Energy Rate (\$/kWh)	0.08	0.12	0.16
TES C-rate Limit (1/h)	2	4	4 ^b
TES Capital Cost (\$/kWh) ^c	50	100	150
TES Lifetime (yr)	10	15	20

^a We consider cases where the demand charge is assessed all year or only in summer months

3. Results and discussion

The results of this study are divided into two parts: 1) load duration curves for each scenario for visualization purposes and 2) potential synergies between batteries and thermal energy storage by analyzing peak demand reduction potential for different systems. The second part looks at potential synergies by calculating utility cost savings, equivalent full cycles for the battery, total annualized cost savings, and other variables.

3.1 Load profiles and load duration curves

The load duration curves shown here are helpful to gain intuition about the relative advantages and disadvantages of BES and TES during different months of the year, particularly in observing the degree to which the thermal load coincides with the peak metered load. It is also necessary to understand the shape of the profiles in the different scenarios when interpreting the plots in the second section of this study's results.

^b 4C is the maximum possible discharge C-rate for simulations involving 15-minute timesteps

^c We also consider a special case where the TES capital cost equals the BES capital cost (\$600/kWh_e)

Load duration curves (Figure 6) make the visual comparison between different scenarios simpler than time-series data (compare with Figure 3 and discussion in Section 2.3) due to the sorting from highest to lowest. The inset figure on top right shows the first 144 hours of the duration curve, which corresponds to the annual peak demand for each scenario. The peak demand for the baseline building is 1,100 kW. Adding fast-charge EVs increases this peak demand by 318 kW (28%), while adding PV reduces it by 33 kW (3%). Even though the nominal power generation capacity of the PV is over half of the maximum power, the reduction in the peak by adding PV is limited because the peak PV generation is not coincident with the peak building demand. Similarly, adding PV to the B+EV scenario reduces peak demand by 66 kW (5%), again due to the noncoincident nature of PV and the random nature of the EV charging. Although EV charging happens during operating hours for the big-box retailer, the peak EV load does not necessarily coincide with the peak solar output (around noon) nor at the time of maximum thermal load (around 1500 hours).

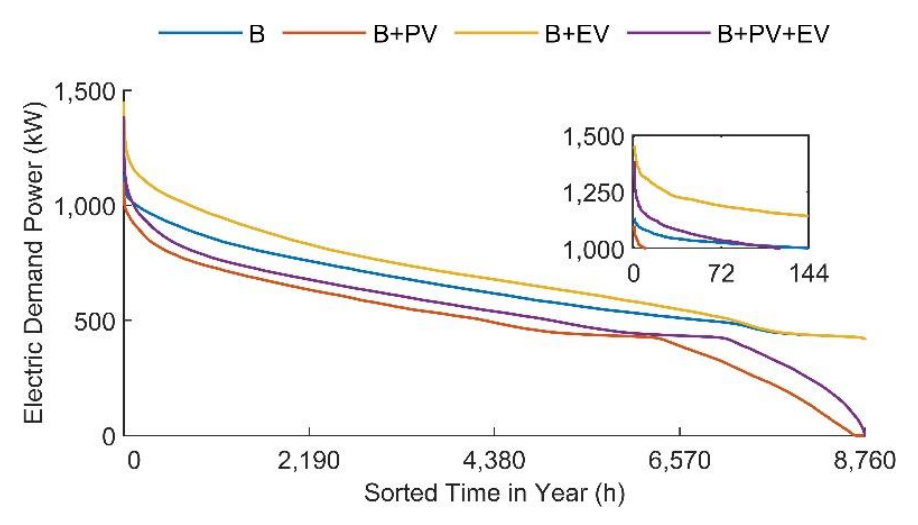


Figure 6: Annual load duration curve for the four scenarios; zoomed insert figure on top right shows the first 144 hours of the duration curve

Figures 7 and 8 show the load duration curves for July and January along with the thermal and nonthermal load profiles for each of the four scenarios ((a)-(d)). The curves showing the electric power demand from thermal loads in each monthly load duration curve differ slightly since each building has a different total load duration curve. For the baseline building, the air conditioning load in January is only 13% of the total peak electric load, whereas in July it is 40% of the total peak electric load. This ratio depends on local weather and building type but shows a well-known trend: higher cooling electricity loads occur in summer due to higher temperatures and mechanical

cooling. When adding extreme-fast EV charging, the role of cooling load on the peak demand is reduced to 4% and 29%, respectively.

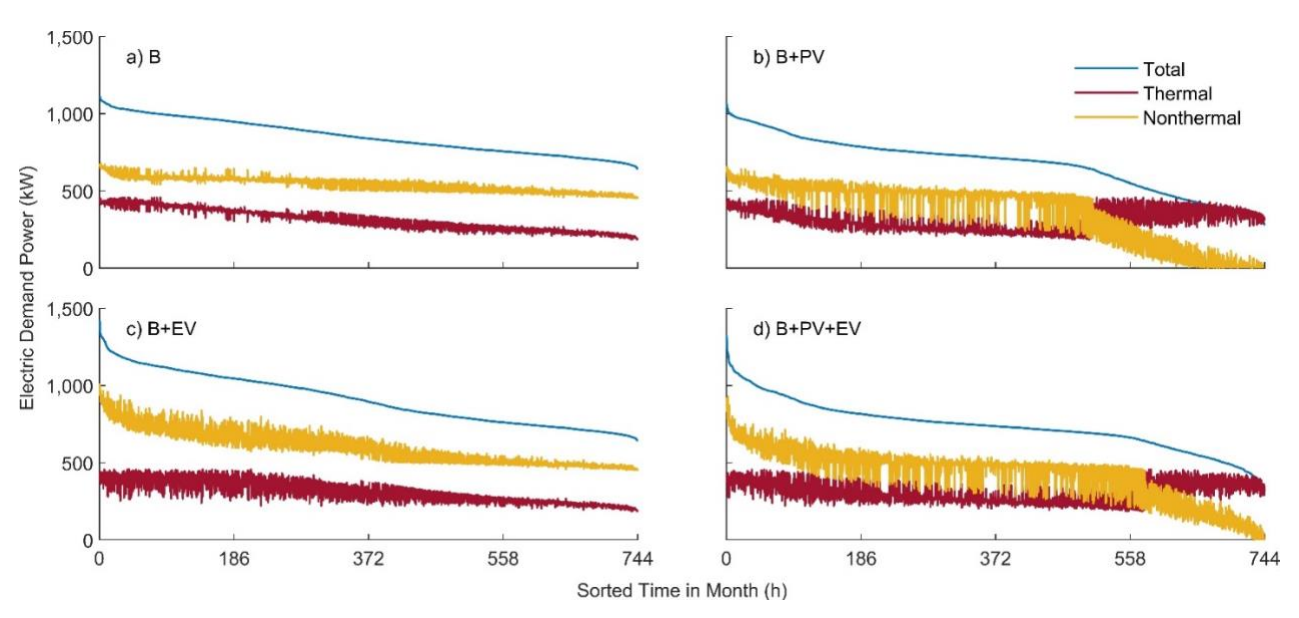


Figure 7: July load duration curves showing curves for total electric load (Total), concurrent thermal loads (Thermal), and concurrent nonthermal loads (Nonthermal) for: (a) baseline building, (b) building with PV, (c) building with EV, and (d) building with PV and EV

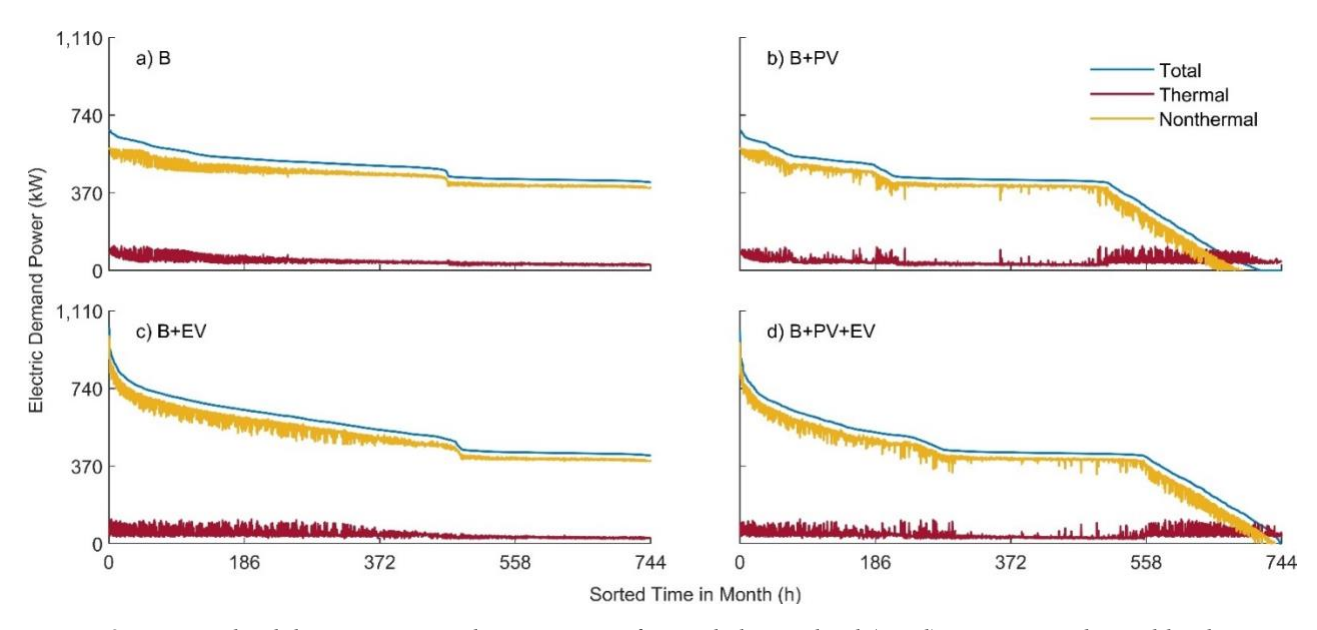


Figure 8: January load duration curves showing curves for total electric load (Total), concurrent thermal loads (Thermal), and concurrent nonthermal loads (Nonthermal) for: (a) baseline building, (b) building with PV, (c) building with EV, and (d) building with PV and EV

In Figure 7(a) for the baseline building in summer, the thermal load is strongly correlated with the total load, with these two curves being relatively "parallel." This indicates that the nonthermal loads are relatively constant (yellow curve is relatively flat at 500-700 kW). In contrast, Figure 8(d) shows that for the B+PV+EV scenario in winter months, the thermal load is not strongly correlated to the total load. The nonthermal load increases at different timesteps by EV charging and is reduced at other timesteps by PV. The range of nonthermal loads as shown in yellow in Figure 8(d) is close to 0-1000 kW. See Appendix B for additional discussion on how the load profile shapes influence the useful storage capacities for BES, TES, and hybrid systems.

3.2 Annual performance and annualized cost savings of hybrid storage systems

There are five primary outputs explored in the figures below, based on the analytical method described above: utility cost savings, annualized total cost savings, and battery discharge characteristics—specifically annual cycling, and the maximum and average discharge C-rates. Although not presented here, similar plots could be constructed for the TES discharge characteristics.

Figure 9 shows annual results for the B+PV+EV scenario. The top two plots, (a) and (b), show the annual utility cost savings and battery equivalent full cycles. Plots (c) and (d) show annual cost savings after accounting for the storage systems' capital costs. In plot (c) the TES cost is equal to the battery cost, while plot (d) shows the outcome when TES is six times less expensive than batteries. Finally, plots (e) and (f) show the maximum and average C-rate for the battery, respectively. In all cases, the x-axis shows increasing TES energy capacities while the y-axis shows increasing BES energy capacities. The contours are colored according to the variable of interest, as indicated by each plot's color bar.

For this scenario, consider different combinations of a 600 kWh_e hybrid system shown by the black line. The utility cost savings potential is the same for a battery-only system (indicated by the circle) or a battery / TES size of 300 kWh_e / 300 kWh_e (indicated by the star). Selecting a larger TES size and smaller battery size will lead to lower battery cycling (Figure 9 (b)), but will also lower the demand savings potential (Figure 9(a)). The system performance of a TES-only 600 kWh_e system (indicated by the square) achieves about half of the utility cost savings.

Figure 9(c) shows the annualized cost savings when BES and TES have the same capital costs. Any combination of BES and TES along the line between the standalone BES (circle) and hybrid

system (star) will provide the maximum (or very close to the maximum) annualized cost savings because the storage types have the same capital costs and load shaving potential. However, the maximum cost savings is not achieved for hybrid systems with a larger TES or standalone TES (points along the line between the star and square). Figure 9(d) shows the annualized cost savings when the capital cost of TES is lower than BES. The maximum cost savings region (yellow) includes larger TES sizes when the TES is much less expensive than the battery, but to achieve the maximum savings requires a battery size of at least 200 kWh_e because the thermal storage can provide only limited peak shaving without a battery to address the nonthermal load. For the case of lower TES costs (Figure 9(d)), the range of TES sizes from 300 to 1,200 kWh_e result in roughly the same annual cost savings once paired with a battery of about 300 kWh_e. For the smaller TES capacities, the initial cost of purchasing the hybrid storge system is smallest, as is the utility cost savings. On the larger side, the initial investment cost is higher, but the added TES capacity provides more utility cost savings to offset the higher cost.

The bottom two plots show the battery C-rate's maximum (Figure 9(e)) and average (Figure 9(f)) values over the course of the year. As the battery size is reduced, the C-rate increases. For a given TES system, small battery capacities lead to high C-rates (and lower power capacities). This explains why the smaller battery capacities (<300 kWh_e) for the hybrid system are less beneficial, at least for this scenario.

Taken as a whole, Figure 9 can be used to compare the three systems indicated by the circle (all battery), square (all TES), and star (hybrid system). A 600 kWh_e battery achieves 83% of the maximum possible peak reduction and experiences around 170 equivalent full cycles each year. It would also have a maximum C-rate of 0.85 and an average C-rate of 0.04. The hybrid system achieves the same peak demand reduction but lowers the equivalent full cycles for the battery to 83. The maximum C-rate also increases to 1.0, but the average stays about the same.

This shows that the hybrid system, even for a case where TES and batteries have the same capital cost, may be preferred because it lowers the battery equivalent full cycles by over 50%. This could extend the life of the battery and improve economics. More likely, the TES will have lower capital costs, making the economics even more favorable (Figure 9(d)).

These results are consistent with a couple of observations made by others in the literature. Firstly, our literature review cites a variety of studies which suggest that, subject to a wide range of

assumptions, scenarios, and system types, utility cost savings of an accurately sized hybrid system may range anywhere from 10-25% (e.g., [24]). In the scenario considered here, we see that the pseudo-optimal system reduced utility cost savings around 18%.

Secondly, several studies including Wu et al. [28] and others (e.g., [39]) predict that relatively small batteries are typically optimal for peak shaving. Our algorithm can be used for standalone system analysis by looking along the x-axis (TES only) and y-axis (BES only) of Figures 9 through 12. In the scenario considered in Figure 9, we see that there is a pseudo-optimal battery-only capacity of around 400 kWh (y-axis) which is qualitatively "small" compared with the maximum possible useful battery capacity of around 1,200 kWh, although we predict a higher amount of peak shaving potential than do Neubauer and Simpson [39]. They predict optimal peak shaving of only 3% for a standalone battery while our study predicts closer to 20%. This is likely due to this scenario's inclusion of EV loads which tend to increase the amount of peak demand reduction potential of a given unit of energy storage. In fact, as discussed below, Figure 11(a) and 11(b) indicate an optimal battery size much less than 400 kWh for the building-only scenario.

Finally, some studies (e.g., [5], [26]) discuss how adding TES can achieve similar peak shaving with a smaller battery. For the scenario considered here, to achieve the same peak reduction as a standalone battery, a hybrid system may utilize a battery which has been downsized around 50%. Returning to the Wu et al. study [28], we have expanded upon their findings for a BES-only system to one with both TES and BES, and show that annualized cost savings can be lower with this hybrid system than the BES-only system (Figure 9(d)).

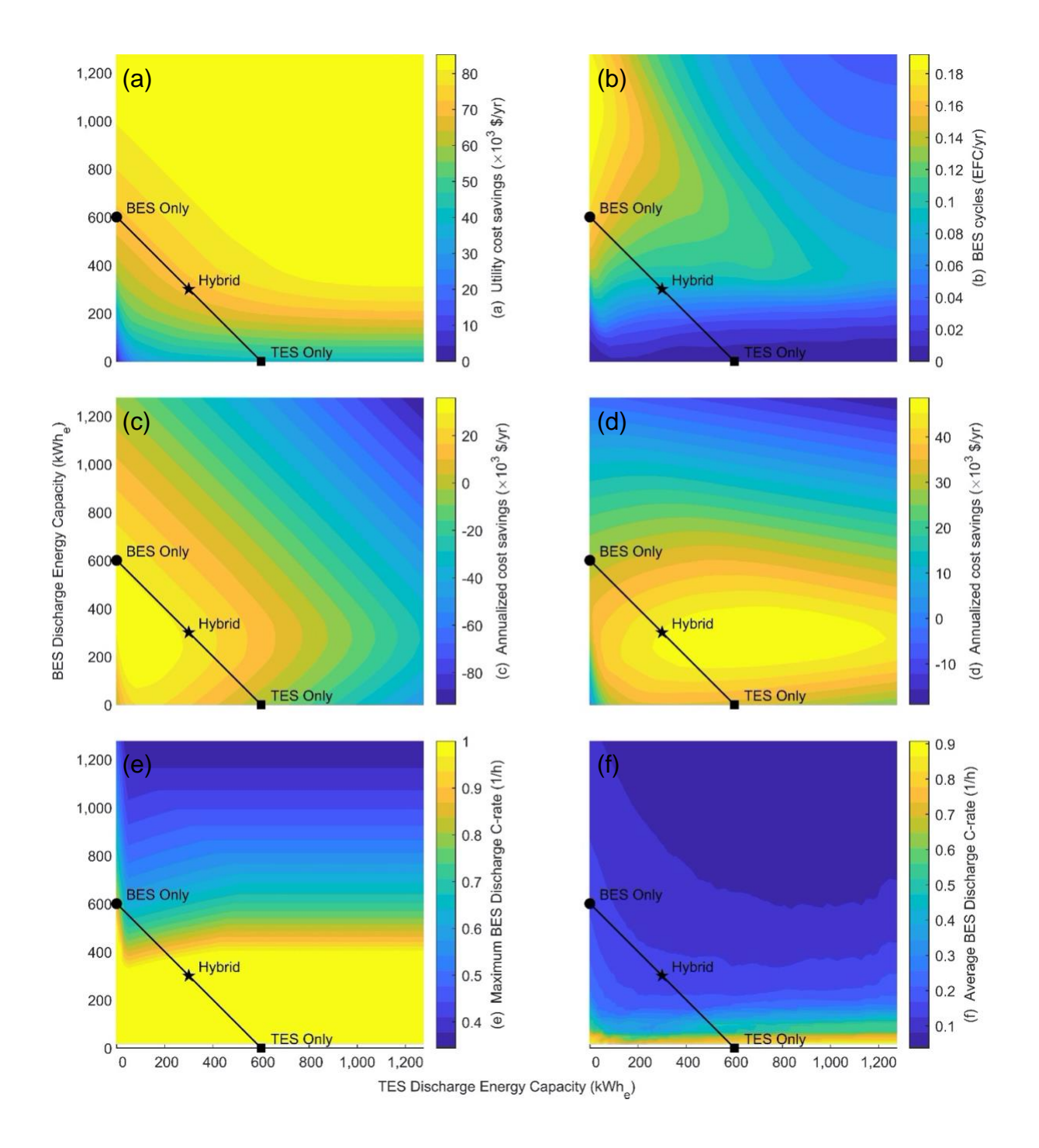


Figure 9: (a) Annual utility cost savings; (b) annual equivalent full cycles (EFC) for battery assuming TES discharge is prioritized; (c) annual total cost savings assuming TES capital expense is equal to BES; (d) annual total cost savings assuming TES capital expense is BES/6; (e) maximum C-rate experienced by battery for any timestep in year; (f) average C-rate experienced by battery for all discharging timesteps plotted for different energy capacities of TES (x-axis) and BES (y-axis) for B+PV+EV scenario; the black line shows a constant storage capacity of 600 kWh_e.

Utility Cost Savings comparing two scenarios and two utility rate structures

In Figure 10, the utility cost savings are shown for four different examples, varying the scenario between Building only and B+PV+EV scenarios, as well as varying the utility rate structure between summer only demand charges and charges assessed for all months in the year.

In Figure 10(a), there is no meaningful difference between a BES system or a TES system—a hybrid system of any capacity, regardless of the fraction from BES or TES yields the same demand reduction potential. This is because demand charges are assessed only in the summer when the cooling load is high. Furthermore, the variations in the load profile are primarily from the thermal load (i.e., the nonthermal load is more consistent). Recall that for a demand charge assessed on all timesteps, a flat load cannot be beneficially shifted. Demand savings in this case require load variations so that charging and discharging timesteps approach a flat-line condition. Although the BES has an imposed C-rate limit, this limit is only relevant for small capacity batteries, and thus does not appreciably change the contours.

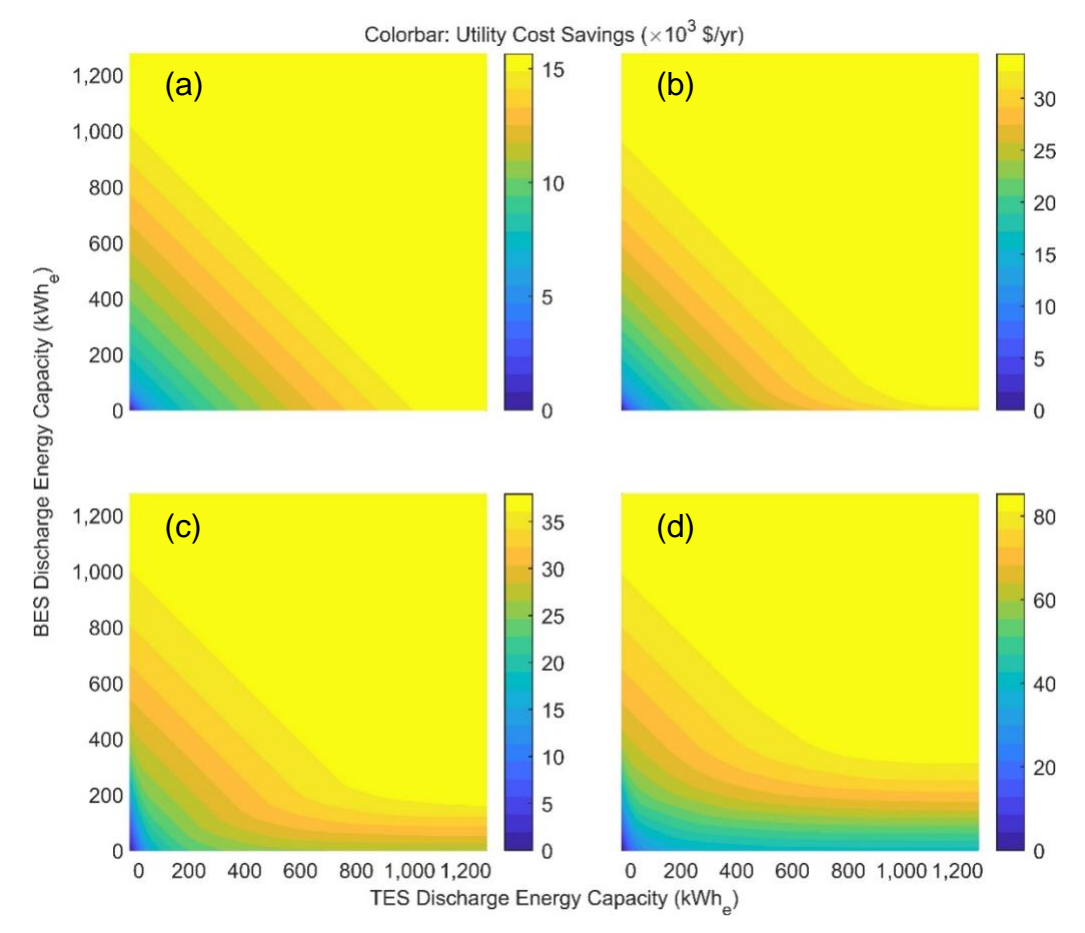


Figure 10: Utility cost savings in thousands of dollars per year for (a) building only with summer demand charges, (b) building only with annual demand charges, (c) building with PV and EV charging stations with summer demand charges, and (d) building with PV and EV charging stations with annual demand charges. Note that the range shown by the colorbar differs for each plot.

By comparison, the building only scenario with demand charges assessed for all months in the year, Figure 10(b), shows that a small battery is required to achieve the maximum possible demand reduction, even for very large TES-only systems. Although the effect is small, there are at least some timesteps in which a nonthermal load during winter months must be shaved. The effect is small because it remains true that for the building-only scenario, most of the load variation in this climate is due to cooling loads, even for winter months. Comparing Figure 10(a) and Figure 10(b) also shows that the maximum possible utility cost savings is approximately double when demand charges are assessed annually instead of during summer months only. This implies that all months in the year have similar variations, even if the absolute value of the load is higher during the summer months (see Figure 3).

The plots in Figure 10(c) and (d) show the B+PV+EV scenario for the summer and annual demand charge examples, respectively. In both cases, the presence of high nonthermal loads from the EV charging and the decrease in the net load during the day from PV when the cooling load is higher results in a greater requirement from a battery to achieve the maximum amount of utility cost savings. In the case of summer demand charges, the minimum battery required is around 200 kWh; however, including demand charges during winter months increases the minimum required battery size to 400 kWh.

Each of the four plots in Figure 10 show similar trends in the top left (large BES, small TES): a quasi-parallel negative slope, indicating that incrementally adding either BES or TES yields the same incremental peak demand reduction. For these smaller TES systems, the thermal load has not fully been met by the thermal energy storage, thus, BES and TES are essentially interchangeable in their ability to reduce peak demand (recall that we have assumed that either storage system has the same electrical round-trip efficiency).

The bottom right corner of the four plots in Figure 10 (small BES and large TES) deviate from this quasi-parallel slope. This shows the limitations of TES—all thermal loads have been met by TES and further peak demand shaving requires a BES. Thus, scenarios involving either winter demand charges or significant nonthermal loads from EV charging show the requirement for at least some battery.

Annualized Cost Savings comparing two scenarios and two utility rate structures with equal capital costs

Figure 11 shows the annualized total cost savings for the same four examples as Figure 10 when the TES capital cost equal the BES capital cost at 600 \$/kWhe. Since there is no difference between the cost of either component in a hybrid system, the plots' contours/trends are closely related to the utility cost savings plots. The plots in Figure 11(a) and (b) show that a BES-only, TES-only, or hybrid system can all achieve roughly the same total cost savings for a given system capacity. The requirement for a small battery in the annual demand charge example, plot (b), is revealed by the slight curve near the x-axis. Plot (c) shows that for small batteries without TES (i.e., bottom left corner on y-axis), the C-rate limit reduces the cost savings compared with adding a small TES, which can discharge at the timestep-limited rate of 4C. However, this effect is small, and the contour shapes in plots (a)-(c) are all very similar. By contrast, for the example involving the

B+PV+EV scenario with demand charges assessed at all times (Figure 11(d)) it is impossible to reach the maximum total cost savings without at least some battery capacity, consistent with findings from the utility costs savings discussion. As shown in Figure 11, the annualized cost savings are often negative, except for very small systems. This indicates that the assumed high capital costs (\$600/kWh_e) are preventing larger sizes of storage from being cost effective. However, TES is often less expensive than BES, which we explore next.

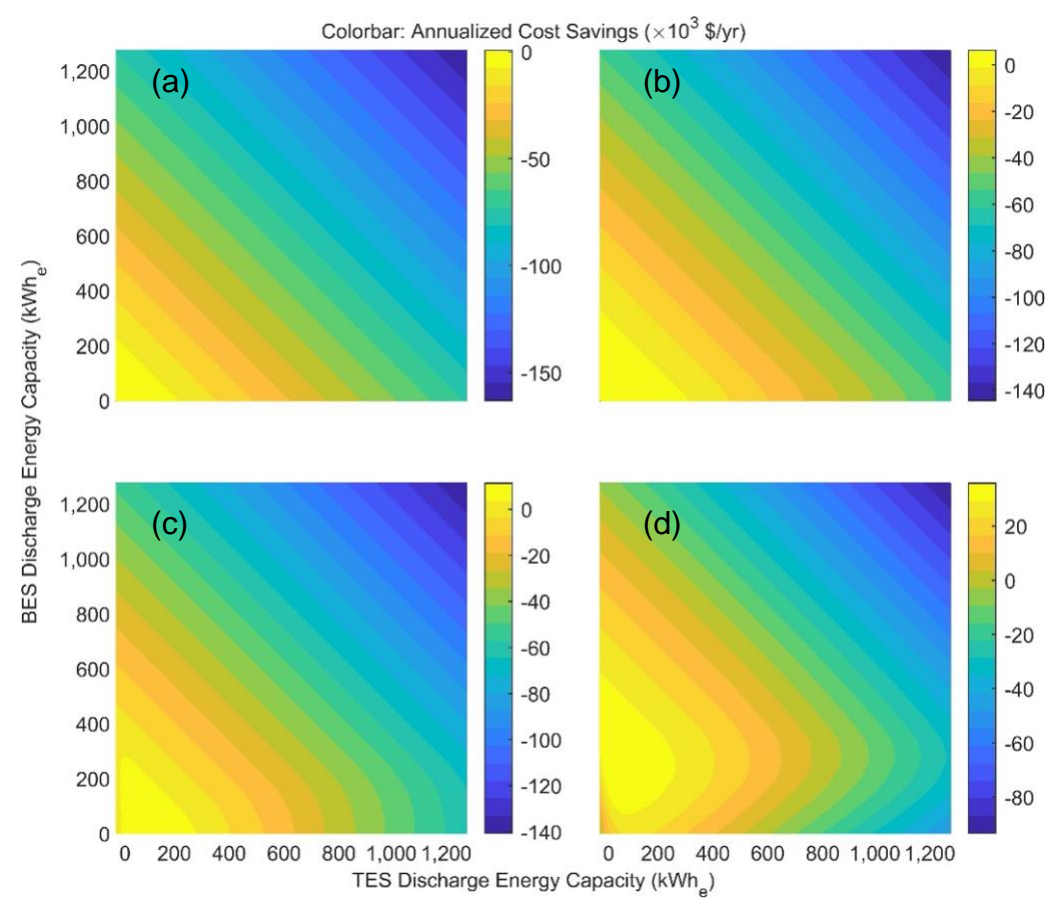


Figure 11: Annualized total cost savings in thousands of dollars per year when TES has the same capital cost as BES for (a) building only with summer demand charges, (b) building only with annual demand charges, (c) building with PV and EV charging stations with summer demand charges, and (d) building with PV and EV charging stations with annual demand charges

Annualized Cost Savings comparing two scenarios and two utility rate structures with different capital costs

Figure 12 shows the annualized cost savings when the TES capital cost is six times lower than the BES. In all four cases, the pseudo-optimal system is expected to be a TES, perhaps with a small battery as needed. For example, as we saw in Figure 10(a), the BES and TES operate in an essentially equivalent manner if the thermal load is high and the demand charge is only assessed during summer months. Therefore, either system will yield the same total cost savings when capital costs are the same (Figure 11(a)). But here, TES is strongly preferred because of its lower capital cost. The full range of TES sizes offer roughly the same total savings because as the system capacity increases, it can accomplish more demand shaving. Thus, the capital costs increase but so do the utility cost savings. That a battery increases total cost savings at only very small capacities is consistent with other studies (e.g., [39]). Expensive storage systems are typically most beneficial when the capacity (and therefore capital cost) is low. The small system only addresses the highest spikes in the load, which yield the greatest utility cost savings per unit of storage.

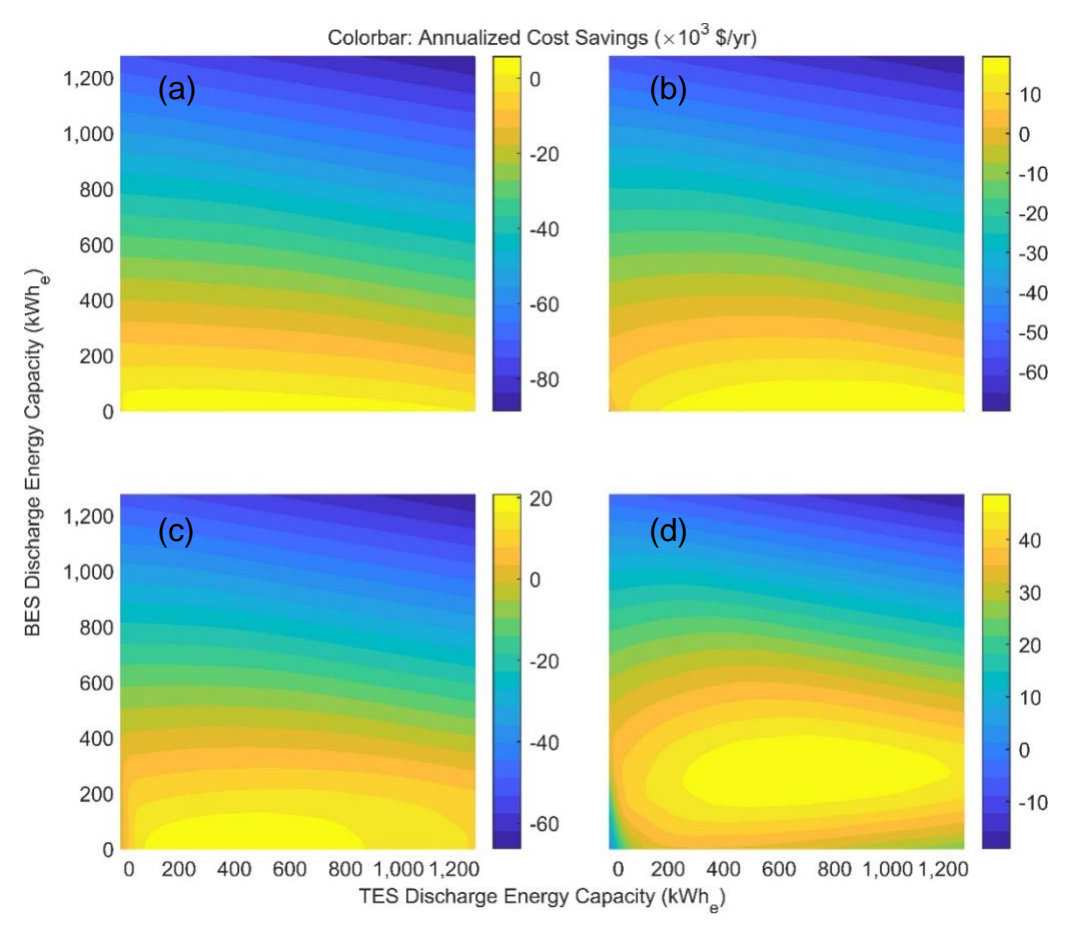


Figure 12: Annualized total cost savings in thousands of dollars per year when TES has a lower capital cost than BES for (a) building only with summer demand charges, (b) building only with annual demand charges, (c) building

with PV and EV charging stations with summer demand charges, and (d) building with PV and EV charging stations with annual demand charges

Figure 12(c) shows the savings for the B+PV+EV scenario with summer demand charges. This plot similarly suggests that a small battery, if one is used at all, is preferred. If no battery is included, the system cannot achieve the maximum peak demand reduction, but the lower cost of TES makes it the most cost effective. Unlike the plots in Figure 12(a) and (b), the range of TES capacities offering the maximum benefit is limited to 850 kWhe. This is the point where increasing the TES capacity would not achieve additional demand reduction in the absence of a battery. This also corresponds to the TES capacity where the quasi-parallel behavior "flattens out" in Figure 10(c).

Finally, we see in Figure 12(d) the same plot as Figure 9(d). This is the annualized cost savings for annual demand charges in the B+PV+EV scenario when TES is significantly less expensive than BES. As discussed previously, adding EVs and winter demand charges make a battery more beneficial. Therefore, in plot (d), to achieve the maximum possible benefit always requires at least a moderate amount of battery capacity. Although the minimum BES capacity required to achieve the maximum demand reduction is about 400 kWh_e (Figure 10(c)), the maximum annual cost savings are around 200 kWh_e since the TES has lower capital costs.

3.3 Sensitivity analysis

Here we explore how the assumed values impact our results when nominal values vary according to Table 1 (typically by \pm 50%). Figure 13 shows the fraction of the pseudo-optimal storage system from TES, based on the system that gives the highest annualized cost savings for each scenario. A value of 1.0 means the pseudo-optimal system is a standalone TES, and a value of 0 means that the selected system is a standalone battery. Figure 13(a) and (b) show the building only scenario with summer-only and annual demand charges. Figure 13(a) shows that all variations of assumed values result in the same TES fraction of 1.0 for the example case analyzed. The relatively constant nonthermal load and the high thermal load make TES the preferred system across all assumptions in this case.

There is also very little variation in Figure 13(b), in which demand charges are assessed for all months of the year. Although thermal loads are smaller in winter, they nevertheless account for

most daily variations, which is important for energy storage systems so that they can fill the valleys and reduce the peaks to lower the overall peak demand. Thus, TES remains favorable to BES with almost no variation across the assumptions considered in this sensitivity analysis.

In the bottom two cases (Figure 13(c) and (d)), the scenario includes PV and EV charging stations. Thus, variations in the load profile have significant contributions from both thermal and nonthermal loads. Here we see greater sensitivity to variations in the assumed parameters. In frame (c), most assumptions still yield a pseudo-optimal system with 100% TES. This is because demand charges are only assessed in summer months, when the thermal load is sufficiently high. The two parameters that lead to a different outcome are the "low" BES capital cost (yellow square) and the "high" demand charge (green star). Unlike frame (a), frame (c) involves EV charging which tends to increase the potential for batteries to provide a net benefit. Thus, when the capital cost of batteries is lowered to \$300/kWhe, the pseudo-optimal system has a TES fraction of 0.8, compared to 1.0 for the nominal capital cost. Increasing the demand charge tends to increase the value of maximizing peak demand reduction, which increases the potential benefit of all storage types and especially batteries, since they are not limited to meeting thermal loads. Thus, in the case where the demand charge has been increased to "high", the pseudo-optimal system has a mix of TES and BES.

Nearly every set of inputs considered for Figure 13(d) yielded a pseudo-optimal system as some hybrid with a TES fraction between 60% and 80%. The one instance where a standalone TES (i.e., TES fraction is 100%) is favored is when the demand charge is reduced to its "low" value of 7.5 \$/kW. When demand charges are reduced, the potential benefit of storage systems for peak shaving is also reduced. Thus, the point at the green star on frame (d) corresponding to 100% TES with a lower demand charge is suggesting that the optimal system is small (since only a small amount of peak demand reduction is cost effective), and the TES can handle all peak demand reduction. Thus, the more expensive battery is avoided. All other instances considered by this sensitivity analysis yield a hybrid system.

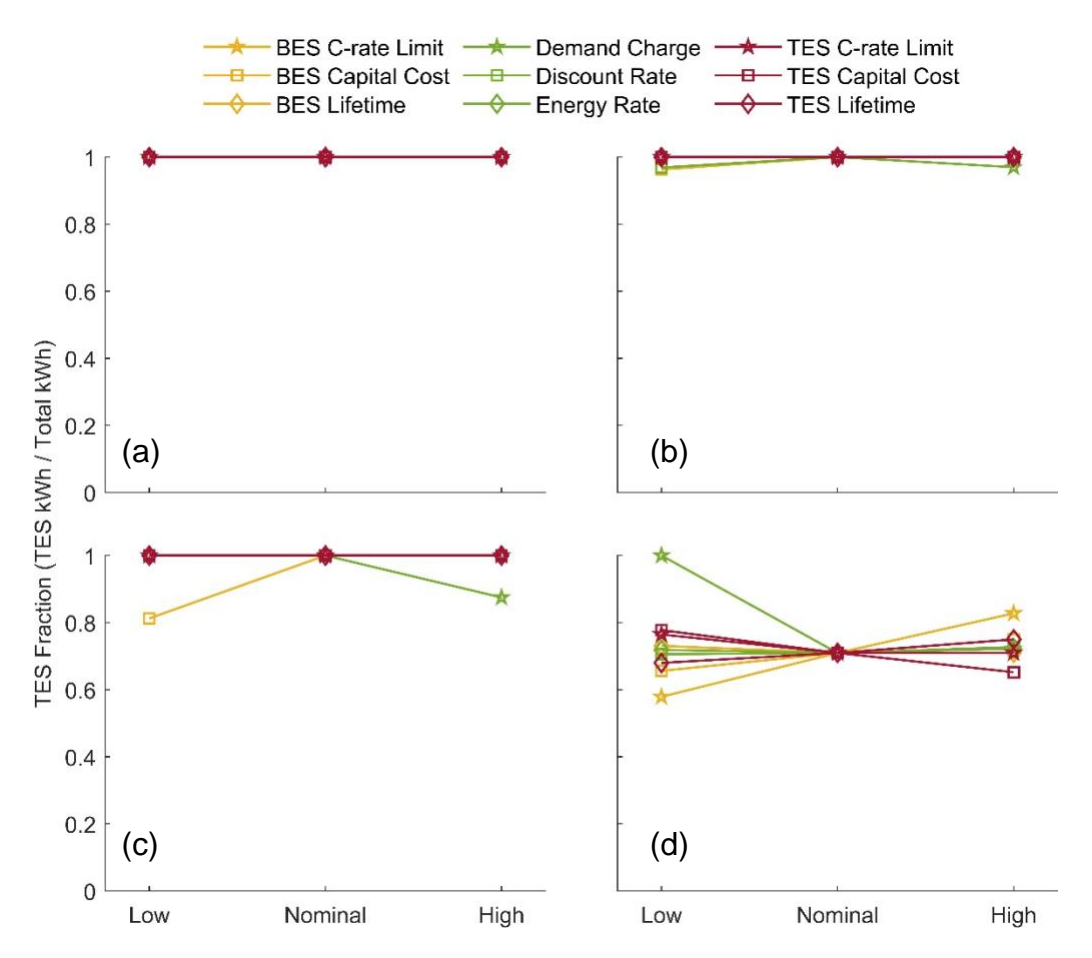


Figure 13: Sensitivity plots showing the TES fraction of the storage system with the maximum annualized cost savings for (a) building only with summer demand charges, (b) building only with annual demand charges, (c) building with PV and EV charging stations with summer demand charges, and (d) building with PV and EV charging stations with annual demand charges. The meaning of low, nominal, and high values is given in Table 1.

Of these results, the TES fraction is most sensitive to the TES capital cost (red squares with a "negative slope") and the BES C-rate limit (yellow stars with a "positive slope"). The TES fraction is inversely proportional to the TES capital cost. Nevertheless, the pseudo-optimal system for the low, nominal, and high TES capital costs is a hybrid with a large contribution from TES with at least some battery to meet the high nonthermal loads.

Finally, we consider the sensitivity to the BES C-rate limit. The sensitivity plot presented in frame (d) shows that as the BES C-rate limit is reduced, the fraction from BES is increased. This indicates that the BES must contribute some amount of discharge power. If the BES C-rate limit is low, then a BES which would otherwise have sufficient discharge energy capacity will not have enough discharge power to shave the nonthermal loads to maximize annualized cost savings. Thus, a larger

energy capacity battery (and therefore larger absolute discharge power) will be selected, increasing the BES fraction and reducing the TES fraction. The opposite is also true: a higher relative power requires a smaller battery to meet a particular absolute discharge power.

This sensitivity analysis shows that, regardless of variations in the inputs assumed, our main conclusion remains—there exist potential synergies between batteries and thermal energy storage, for the four building scenarios in the hot climate simulated here, due to their comparative advantages and disadvantages at meeting different kinds of loads with different performance and cost characteristics.

4. Conclusions

This study proposes a simple method for sizing a hybrid battery/TES system. We calculate the possible load reduction and annualized cost savings for a hybrid system of different sizes using a binary search approach. We use this method to investigate tradeoffs and synergies of a hybrid battery/TES system for a retail grocery store in Phoenix, AZ, using simulated load profiles. This method shows how thermal storage can be used synergistically with a battery, and how these hybrid systems can be preferred to a standalone battery-only or TES-only system. The four key takeaways are:

- 1) Adding batteries to a TES system can increase the total system's load shaving potential (and increase TES utilization for peak demand reduction). This is particularly true when the building has onsite PV generation or EV charging, which add significant variability to the load shape.
- 2) Adding TES to a battery system can improve economics since TES often has a lower capital cost, and because it can significantly lower battery cycling, extending the battery life.
- 3) In the climate analyzed in this study, which has a large cooling load, the pseudo-optimal hybrid design is often some combination of thermal and battery storage, and rarely only a battery-only or TES-only system.
- 4) If demand charges are assessed only in the summer, the pseudo-optimal system will have a greater fraction of TES for this cooling case, even in scenarios with significant nonthermal loads from EV charging. Contrarily, utility rate structures in which demand charges are assessed on all months in the year or climate zones with milder summer

temperatures increase the likelihood that a battery will be beneficial or required to reach high demand reduction.

In the future, this model could be expanded to allow for multiple demand charges (\$/kW) with or without time-of-use electricity (\$/kWh) rates. Future investigations could also analyze different building types, climates, EV charging scenarios, and investigate the impacts of different EV, PV, and energy storage performance and cost parameters. Future work could also investigate how a similar method could be adapted to minimize CO₂ emissions, rather than utility or total annualized costs, to help mitigate climate change. For this study and any future study, controls remain a challenge for hybrid systems. Achieving the potential synergies described in this study depend on developing control strategies that can obtain the predicted peak demand reduction, which assumes an ideal dispatch algorithm.

CRediT authorship contribution statement

Matthew Brandt: Methodology, Software, Writing-Original Draft, Visualization. Jason Woods: Conceptualization, Writing-Review and Editing, Supervision, Funding Acquisition. Paulo Cesar Tabares-Velasco: Conceptualization, Writing-Review and Editing, Supervision

Acknowledgments

This work was authored by the National Renewable Energy Laboratory, operated by Alliance for Sustainable Energy, LLC, for the U.S. Department of Energy (DOE) under Contract No. DE-AC36-08GO28308. Funding was provided by the DOE's Office of Energy Efficiency and Renewable Energy, Building Technologies Office, and Vehicles Technologies Office. The views expressed in the article do not necessarily represent the views of the DOE or the U.S. Government. The U.S. Government retains and the publisher, by accepting the article for publication, acknowledges that the U.S. Government retains a nonexclusive, paid-up, irrevocable, worldwide license to publish or reproduce the published form of this work, or allow others to do so, for U.S. Government purposes. The authors also acknowledge Ian Doebber and Maddy Gilleran for their valuable contributions.

References

- [1] "How much energy is consumed in U.S. residential and commercial buildings?," U.S. Energy Information Administration (EIA), May 2019. https://www.eia.gov/tools/faqs/faq.php?id=86&t=1 (accessed Jan. 17, 2020).
- [2] "Colorado EV Plan 2020 | Colorado Energy Office." https://energyoffice.colorado.gov/zero-emission-vehicles/colorado-ev-plan-2020 (accessed Sep. 30, 2020).
- [3] "Zero-Emission Vehicles." https://www.cpuc.ca.gov/zev/ (accessed Sep. 30, 2020).
- [4] H. Chen, T. N. Cong, W. Yang, C. Tan, Y. Li, and Y. Ding, "Progress in electrical energy storage system: A critical review," *Progress in Natural Science*, vol. 19, no. 3, pp. 291–312, Mar. 2009, doi: 10.1016/j.pnsc.2008.07.014.
- [5] L. Hu, Y. Liu, D. Wang, and J. Liu, "Battery Capacity Reduction for Stand-Alone PV Air Conditioner by Using Curtailed Electricity to Store Chilled Water as a Backup," in Proceedings of the 11th International Symposium on Heating, Ventilation and Air Conditioning (ISHVAC 2019), Singapore, 2020, pp. 609–617. doi: 10.1007/978-981-13-9528-4 62.
- [6] G. Comodi, F. Carducci, J. Y. Sze, N. Balamurugan, and A. Romagnoli, "Storing energy for cooling demand management in tropical climates: A techno-economic comparison between different energy storage technologies," *Energy*, vol. 121, pp. 676–694, Feb. 2017, doi: 10.1016/j.energy.2017.01.038.
- [7] C. Luerssen, O. Gandhi, T. Reindl, C. Sekhar, and K. W. D. Cheong, "Levelised Cost of Thermal Energy Storage and Battery Storage to Store Solar PV Energy for Cooling Purpose," presented at the International Solar Energy Society, Sep. 2018. doi: 10.13140/RG.2.2.11361.56166.
- [8] M. Ebrahimi, "Storing electricity as thermal energy at community level for demand side management," *Energy*, vol. 193, p. 116755, Feb. 2020, doi: 10.1016/j.energy.2019.116755.
- [9] H. Lund *et al.*, "Energy Storage and Smart Energy Systems," *International Journal of Sustainable Energy Planning and Management*, vol. 11, pp. 3–14, Oct. 2016, doi: 10.5278/ijsepm.2016.11.2.
- [10] Y. Zhou, S. Cao, J. L. M. Hensen, and P. D. Lund, "Energy integration and interaction between buildings and vehicles: A state-of-the-art review," *Renewable and Sustainable Energy Reviews*, vol. 114, p. 109337, Oct. 2019, doi: 10.1016/j.rser.2019.109337.
- [11] H. Akbari *et al.*, "Efficient energy storage technologies for photovoltaic systems," *Solar Energy*, vol. 192, pp. 144–168, Nov. 2019, doi: 10.1016/j.solener.2018.03.052.
- [12] Y. Chen, P. Xu, J. Gu, F. Schmidt, and W. Li, "Measures to improve energy demand flexibility in buildings for demand response (DR): A review," *Energy and Buildings*, vol. 177, pp. 125–139, Oct. 2018, doi: 10.1016/j.enbuild.2018.08.003.
- [13] S. Al-Hallaj, G. Wilk, G. Crabtree, and M. Eberhard, "Overview of distributed energy storage for demand charge reduction," *MRS Energy & Sustainability*, vol. 5, ed 2018, doi: 10.1557/mre.2017.18.
- [14] K. Faraj, M. Khaled, J. Faraj, F. Hachem, and C. Castelain, "Phase change material thermal energy storage systems for cooling applications in buildings: A review," *Renewable and Sustainable Energy Reviews*, vol. 119, p. 109579, Mar. 2020, doi: 10.1016/j.rser.2019.109579.
- [15] S. Rashidi, H. Shamsabadi, J. A. Esfahani, and S. Harmand, "A review on potentials of coupling PCM storage modules to heat pipes and heat pumps," *J Therm Anal Calorim*, Nov. 2019, doi: 10.1007/s10973-019-08930-1.

- [16] E. Guelpa and V. Verda, "Thermal energy storage in district heating and cooling systems: A review," *Applied Energy*, vol. 252, p. 113474, Oct. 2019, doi: 10.1016/j.apenergy.2019.113474.
- [17] I. Sarbu and C. Sebarchievici, "A Comprehensive Review of Thermal Energy Storage," *Sustainability*, vol. 10, no. 1, p. 191, Jan. 2018, doi: 10.3390/su10010191.
- [18] S. Kahwaji, M. B. Johnson, A. C. Kheirabadi, D. Groulx, and M. A. White, "A comprehensive study of properties of paraffin phase change materials for solar thermal energy storage and thermal management applications," *Energy*, vol. 162, pp. 1169–1182, Nov. 2018, doi: 10.1016/j.energy.2018.08.068.
- [19] A. Arteconi, N. J. Hewitt, and F. Polonara, "State of the art of thermal storage for demand-side management," *Applied Energy*, vol. 93, pp. 371–389, May 2012, doi: 10.1016/j.apenergy.2011.12.045.
- [20] N. A. Aziz, N. A. M. Amin, M. S. A. Majid, and I. Zaman, "Thermal energy storage (TES) technology for active and passive cooling in buildings: A Review," *MATEC Web Conf.*, vol. 225, p. 03022, 2018, doi: 10.1051/matecconf/201822503022.
- [21] Y. Sun, S. Wang, F. Xiao, and D. Gao, "Peak load shifting control using different cold thermal energy storage facilities in commercial buildings: A review," *Energy Conversion and Management*, vol. 71, pp. 101–114, Jul. 2013, doi: 10.1016/j.enconman.2013.03.026.
- [22] W. Hu, C. C. Chai, W. Yang, and R. Yu, "Comprehensive modeling and joint optimization of ice thermal and battery energy storage with provision of grid services," in *TENCON 2017* 2017 IEEE Region 10 Conference, Nov. 2017, pp. 528–533. doi: 10.1109/TENCON.2017.8227920.
- [23] J. Niu, Z. Tian, Y. Lu, and H. Zhao, "Flexible dispatch of a building energy system using building thermal storage and battery energy storage," *Applied Energy*, vol. 243, pp. 274–287, Jun. 2019, doi: 10.1016/j.apenergy.2019.03.187.
- [24] C. J. Meinrenken and A. Mehmani, "Concurrent optimization of thermal and electric storage in commercial buildings to reduce operating cost and demand peaks under time-of-use tariffs," *Applied Energy*, vol. 254, p. 113630, Nov. 2019, doi: 10.1016/j.apenergy.2019.113630.
- [25] D. T. Vedullapalli, R. Hadidi, and B. Schroeder, "Combined HVAC and Battery Scheduling for Demand Response in a Building," *IEEE Transactions on Industry Applications*, vol. 55, no. 6, pp. 7008–7014, Nov. 2019, doi: 10.1109/TIA.2019.2938481.
- [26] D. Wang, L. Hu, Y. Liu, and J. Liu, "Performance of off-grid photovoltaic cooling system with two-stage energy storage combining battery and cold water tank," *Energy Procedia*, vol. 132, pp. 574–579, Oct. 2017, doi: 10.1016/j.egypro.2017.09.745.
- [27] J. Borland, J. Moore, C. Poncho, T. Tanaka, and H. McClure, "\$> 94.5%\$ Reduction in Grid-Buy Electricity and Elimination of AM PM Energy Peaks/Spikes by Optimizing Energy Usage and Integration of Customer Self-Supply Rooftop Solar PV with Electrical Thermal (Hot Cold) Storage Batteries: A Case Study for Residential Hawaii," in 2017 IEEE 44th Photovoltaic Specialist Conference (PVSC), Jun. 2017, pp. 2947–2951. doi: 10.1109/PVSC.2017.8366739.
- [28] D. Wu, M. Kintner-Meyer, T. Yang, and P. Balducci, "Analytical sizing methods for behind-the-meter battery storage," *Journal of Energy Storage*, vol. 12, pp. 297–304, Aug. 2017, doi: 10.1016/j.est.2017.04.009.
- [29] "Maximum demand charge rates for commercial and industrial electricity tariffs in the United States OpenEI DOE Open Data." https://openei.org/doe-opendata/dataset/maximum-

- demand-charge-rates-for-commercial-and-industrial-electricity-tariffs-in-the-united-sta181 (accessed Oct. 15, 2020).
- [30] M. Lanahan, S. Engert, T. Kim, and P. C. Tabares-Velasco, "Rapid visualization of the potential residential cost savings from energy storage under time-of-use electric rates," *Journal of Building Performance Simulation*, vol. 12, no. 1, pp. 68–81, Jan. 2019, doi: 10.1080/19401493.2018.1470203.
- [31] J. Woods, A. Mahvi, A. Goyal, E. Kozubal, A. Odukomaiya, and R. Jackson, "Rate capability and Ragone plots for phase change thermal energy storage," *Nat Energy*, vol. 6, no. 3, pp. 295–302, Mar. 2021, doi: 10.1038/s41560-021-00778-w.
- [32] T. Deetjen, A. Reimers, and M. Webber, "Can storage reduce electricity consumption? A general equation for the grid-wide efficiency impact of using cooling thermal energy storage for load shifting," *Environmental Research Letters*, vol. 13, Dec. 2017, doi: 10.1088/1748-9326/aa9f06.
- [33] M. Gilleran *et al.*, "Impact of electric vehicle charging on the power demand of retail buildings," *Advances in Applied Energy*, vol. 4, p. 100062, Nov. 2021, doi: 10.1016/j.adapen.2021.100062.
- [34] P. Mishra *et al.*, "A Framework to Analyze the Requirements of a Multi-Port, Megawatt-Level Charging Station for Heavy-Duty Electric Vehicle," presented at the 99th Transportation Research Board Annual Meeting, Washington D.C., Jan. 2020.
- [35] E. Y. Ucer, M. C. Kisacikoglu, F. Erden, A. Meintz, and C. Rames, "Development of a DC Fast Charging Station Model for use with EV Infrastructure Projection Tool," in *2018 IEEE Transportation Electrification Conference and Expo (ITEC)*, Jun. 2018, pp. 904–909. doi: 10.1109/ITEC.2018.8450158.
- [36] E. Wood, S. Raghavan, C. Rames, J. Eichman, and M. Melaina, *Regional Charging Infrastructure for Plug-In Electric Vehicles: A Case Study of Massachusetts*. 2017.
- [37] N. DeForest, G. Mendes, M. Stadler, W. Feng, J. Lai, and C. Marnay, "Optimal deployment of thermal energy storage under diverse economic and climate conditions," *Applied Energy*, vol. 119, pp. 488–496, Apr. 2014, doi: 10.1016/j.apenergy.2014.01.047.
- [38] R. Fu, T. W. Remo, and R. M. Margolis, "2018 U.S. Utility-Scale Photovoltaics-Plus-Energy Storage System Costs Benchmark," National Renewable Energy Lab. (NREL), Golden, CO (United States), NREL/TP-6A20-71714, Nov. 2018. doi: 10.2172/1483474.
- [39] J. Neubauer and M. Simpson, "Deployment of Behind-The-Meter Energy Storage for Demand Charge Reduction," National Renewable Energy Lab. (NREL), Golden, CO (United States), Golden, CO, Jan. 2015.

Appendix A. Sizing algorithm to obtain minimum energy and power requirements for target peak shaving

The binary search approach described in Section 2.4.1 is utilized for the sizing algorithm. For this algorithm, and the corresponding results associated with this algorithm presented in Appendix B, the objective is to determine the minimum storage system size needed to achieve a target amount of peak demand reduction.

- A. <u>Determine maximum possible demand reduction</u>: The maximum monthly peak shaving is calculated using the binary search approach. Note that the algorithm will also confirm that utility cost savings are obtained by decreasing the guessed amount of peak shaving if the time of shaving (i.e., sum of all discharging timesteps) exceeds the maximum allowed time of shaving.
- B. Sweep through range of possible values of target peak demand reduction: Using the maximum possible peak demand reduction identified in Step A, Steps C-E are repeated for a range of values of target peak demand reduction between zero and the maximum shaving.
- C. Determine BES energy and power capacities: The BES is sized first by summing the nonthermal loads that exceed the target value of peak demand power for each day in the month. The BES is sized first (and independently of the TES) since nonthermal loads cannot be met by TES. This sizing assumes that the storage system discharge capacity is high enough to deliver all required discharge energy in a day with one full depth of discharge. In some cases, recharging may be possible (such as if there is significant PV creating a "bimodal" profile), and the required minimum energy capacity could be calculated to account for such cycling. The required BES power capacity is equal to the timestep with the highest nonthermal load above the target peak shaving.
- D. <u>Determine TES</u> energy capacity based on <u>BES</u> energy capacity: Although the BES is sized independently of the TES, the minimum required TES depends on the BES capacity. This is because the BES may be useful for meeting loads that would normally be met by TES (e.g., the battery is used to run a chiller), whereas the TES cannot always meet BES loads (e.g., the chiller cannot deliver power for plug loads). Therefore, the TES is sized by finding the day with the maximum required energy of discharge and subtracting the BES capacity calculated in Step B.

E. <u>Update energy capacities to satisfy C-rate limit</u>: The discharge C-rate for each energy storage system is determined using the power and energy capacities calculated in the previous steps. If the calculated C-rate exceeds the physical C-rate limit (imposed as a model input), the energy capacity is increased such that the calculated C-rate is equal to the C-rate limit.

Appendix B. Impact of building load profile on required energy and power of hybrid storage systems (sizing results using algorithm discussed in Appendix A)

The required energy sizes of thermal and battery energy storage for a given target level of peak-demand reduction depend strongly on the load duration curves for each scenario. Sizing is also sensitive to the maximum discharge power required by the battery, as batteries are not well suited for high discharge power. Increasing the discharge power of a battery at a fixed energy capacity can dramatically increase the capital expense [38]. Meanwhile, TES systems are, in this context, less sensitive to the discharge power, since shutting off cooling equipment can fully eliminate thermal electric loads. In fact, an active TES may also indirectly benefit from the advantage of passively storing thermal energy in the building structural materials, as it mitigates the need for high discharge powers for TES.

Figures B.1 and B.2 show how the thermal and battery energy storage size changes depending on the desired peak reduction, for both July and January, including (a) the required storage discharge capacity (kWh_e), (b) discharge power (kW), and (c) maximum required C-rate. The thermal storage is sized to handle as much of the load as possible, with batteries added as soon as thermal storage cannot reduce the peak demand further. The required storage size increases with the desired peak reduction, but it is different depending on the scenario. For example, in July, a 200-kW peak reduction will require 1,000 kWh for the Building, 400 kWh for B+PV, 100 kWh for B+EV, and 75 kWh for B+PV+EV. In all scenarios, this 200-kW peak reduction could come from a battery, thermal storage, or a hybrid system of the specified total system size. For comparison, in January, a 200-kW peak reduction cannot be achieved for the Building, and requires 900 kWh in B+PV, 200 kWh in B+EV and 200 kWh in B+PV+EV. In these scenarios, some of the storage must be from a battery because the thermal storage cannot deliver this level of peak reduction by itself.

The results in Figure B.1 provide other detailed insights into how these hybrid systems perform, discussed below for each building scenario:

Baseline Building (July): For the baseline building scenario (Figure B.1(a)), a battery is not needed for any of the possible peak demand reduction levels. For the maximum peak reduction of 205 kW, the thermal storage would be 1,050 kWh with a power of 205 kW, which is a C-rate of C/5. Lowering the peak reduction increases the C-rate, as this requires reducing the peak during fewer and fewer timesteps. In the extreme, the maximum C-rate is 4C, corresponding to a storage that reduces the peak during only one timestep in the entire month. This is unlikely to be cost effective, since there are fixed costs associated with any energy storage system. Therefore, it is more useful to look at higher levels of peak reduction of around 75 kW, which requires a maximum C-rate of 1C. There are diminishing returns from going to much larger sizes when the demand charge is the dominant component in the utility bill, as each additional kWh of storage shaves less and less peak demand. This is shown in the first plot, where the slope is at first shallow, and then increases rapidly above 75-100 kWh.

<u>B+PV (July)</u>: The load profile when including PV (Figure B.1(b)) can still be flattened using only TES, but there are two key changes. Adding PV shortens the duration (but not the magnitude) of the peak, which means it takes less storage for each kW of peak reduction. This is seen in the energy plots in Figure B.1(a) and (b) where less storage is required for 100 kW of peak reduction (91 kWh) compared to the baseline building only scenario (178 kWh). This is also evident from the load duration curve (Figure 7), which has a sharper peak at the beginning of the curve. The maximum C-rate is also higher for these cases up to 100-kW peak reduction because less capacity is used for each kW of load reduction.

Adding PV also reduces the load in the middle of the day, providing more time to charge the storage and a lower 'flattened' peak that corresponds to the end of the curves in Figure B.1. Again, the load duration curve shows this possibility by the steep drop off at the end of the curve ("tail")—a steeper load duration curve signifies more potential for peak reduction compared to a flat load duration curve. The efficiency of the thermal storage charging in the middle of the day will likely decrease because it is hotter outside (higher required temperature lift), but this effect is not included here.

<u>B+EV (July)</u>: The load profile for the B+EV scenario (Figure B.1(c)) shows larger peak-demand reduction potential than the B+PV scenario because the load duration curve is steeper for the first 75% of the curve, and the absolute peak (1050 kW) is much higher than the Building or B+PV scenarios (~700 kW). Although the peak reduction is larger, the resulting load for the maximum peak reduction (flat load duration curve) is still higher than for the baseline Building or B+PV scenarios.

The C-rate curve is also substantially higher for the B+EV scenario, but it still ends around C/5 for the maximum peak reduction case. This means the storage strategy for the scenarios with EVs could either be a modest capacity with high power, or a modest power with a large energy capacity. For example, it could be a 150-kW / 50-kWh storage (3C) for a 150 kW peak reduction, or a 400-kW / 1200-kWh storage (C/3) for a 400-kW peak reduction. For comparison, a 50-kWh storage for the building-only scenario would provide 50 kW peak reduction (1C).

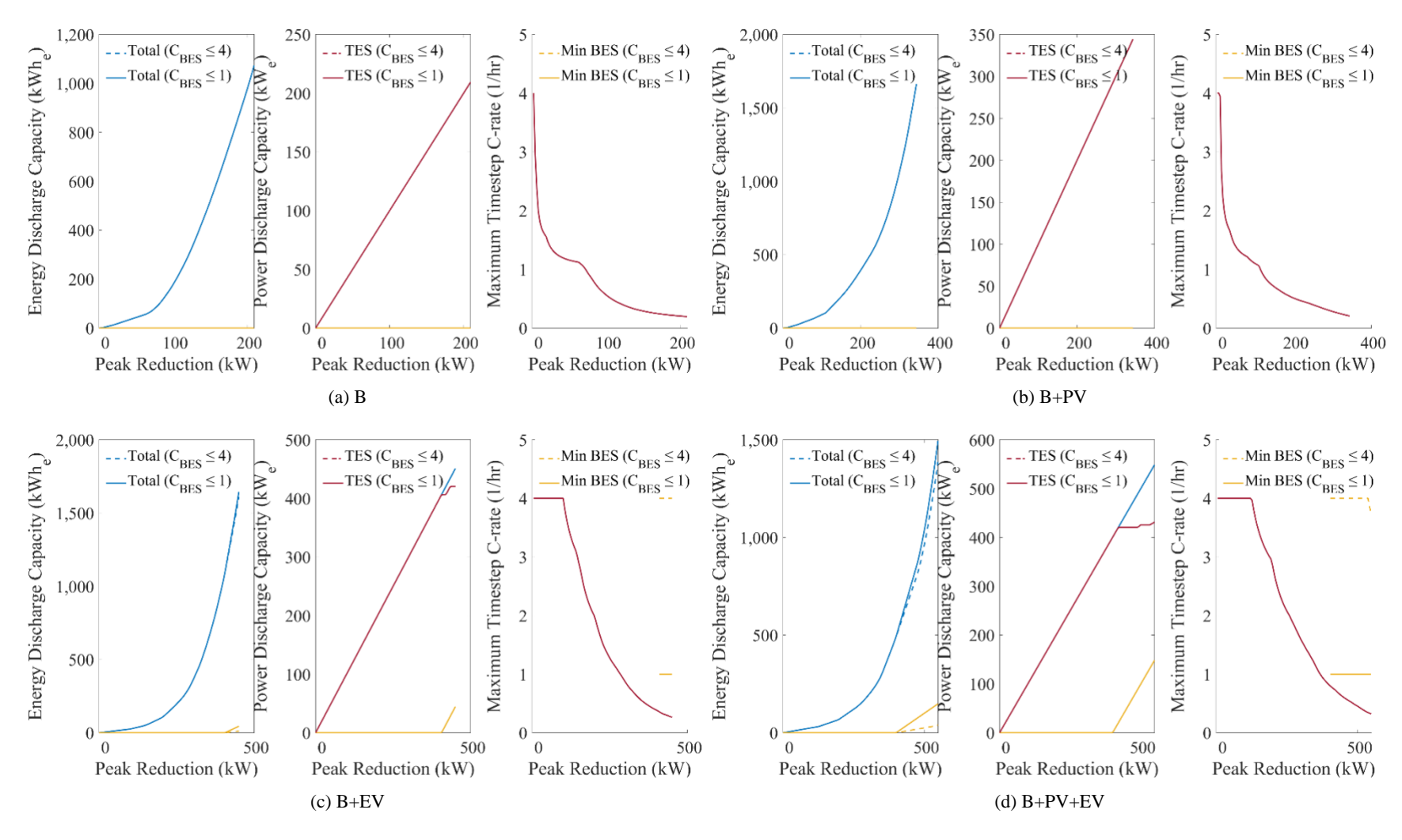


Figure B.1: Impact of peak reduction on required hybrid energy storage capacity (including minimum battery size needed to meet nonthermal loads), required power for both hybrid components, and C-rate for both hybrid components for the four analyzed scenarios: (a) Building only, (b) Building with PV, (c) Building with EV, and (d) Building with PV and EV; Summer design month

The introduction of DC fast charging EV stations also requires battery storage past a 400-kW demand reduction. This 400 kW is the electric demand from air conditioning that corresponds to the peak in the load duration curve. The battery size then increases to shave each additional kW past 400-kW peak reduction. But the size differs depending on whether it is constrained to a 1C or 4C discharge rate. These are shown with the solid and dashed yellow lines, respectively, in Figure B.1(c).

<u>B+PV+EV (July)</u>: Adding PV to the B+EV scenario expands the possible peak-load reduction by allowing more charging during the low 'tail' of electric demand in the load duration curve. Like the B+EV scenario, a battery is required past 400-kW peak demand reduction as TES already meets the thermal loads.

Figure B.2 is laid out the same as Figure B.1, but shows the results for January. Overall, all scenarios require some battery capacity since cooling load is lowest this month of the year and in many locations in the US would be zero, depending on the building type. Results for January would be considerably different if considering a heating TES application, in which a storage media is coupled with a heat-pump or electric-resistance heater for space heating in a colder climate.

<u>Building only (January)</u>: A battery is required to reduce the peak by more than 90 kW, but adding a battery also enables more thermal storage. The battery provides access to more thermal load as we move further to the right on the load duration curve. For a given size of thermal storage, the Crates will generally be lower in January than July because the load is much smaller. Above the 90-kW peak reduction, the C-rate for the battery is high, but a battery was not needed in July because all of the demand reduction could be met by the thermal storage.

<u>B+PV (January)</u>: Like July, adding PV increases the possible peak reduction. The maximum peak reduced by thermal storage is now 100 kW instead of 115 kW for the building-only case, because the PV moved that timestep from the beginning of the load duration curve to the end.

<u>B+EV (January)</u>: Adding DC fast chargers pushes the need for a battery to lower peak reduction levels because some EV charging is non-coincident with the thermal load. This is also true in July, but the ratio of the thermal electric load to the EV load makes this much less common. When adding the battery, the required C-rates are also large because of the short duration and high power

of the EV charging events. The maximum peak demand is also much higher when adding EVs (425 kW), which means there is a need for a much larger battery.

<u>B+PV+EV (January)</u>: Adding PV does not substantially change the shape of these curves compared to the B+EV scenario, but again increases the possible peak demand reduction (500 kW). For this and the B+EV scenario, the battery must be upsized to avoid power above 1C.

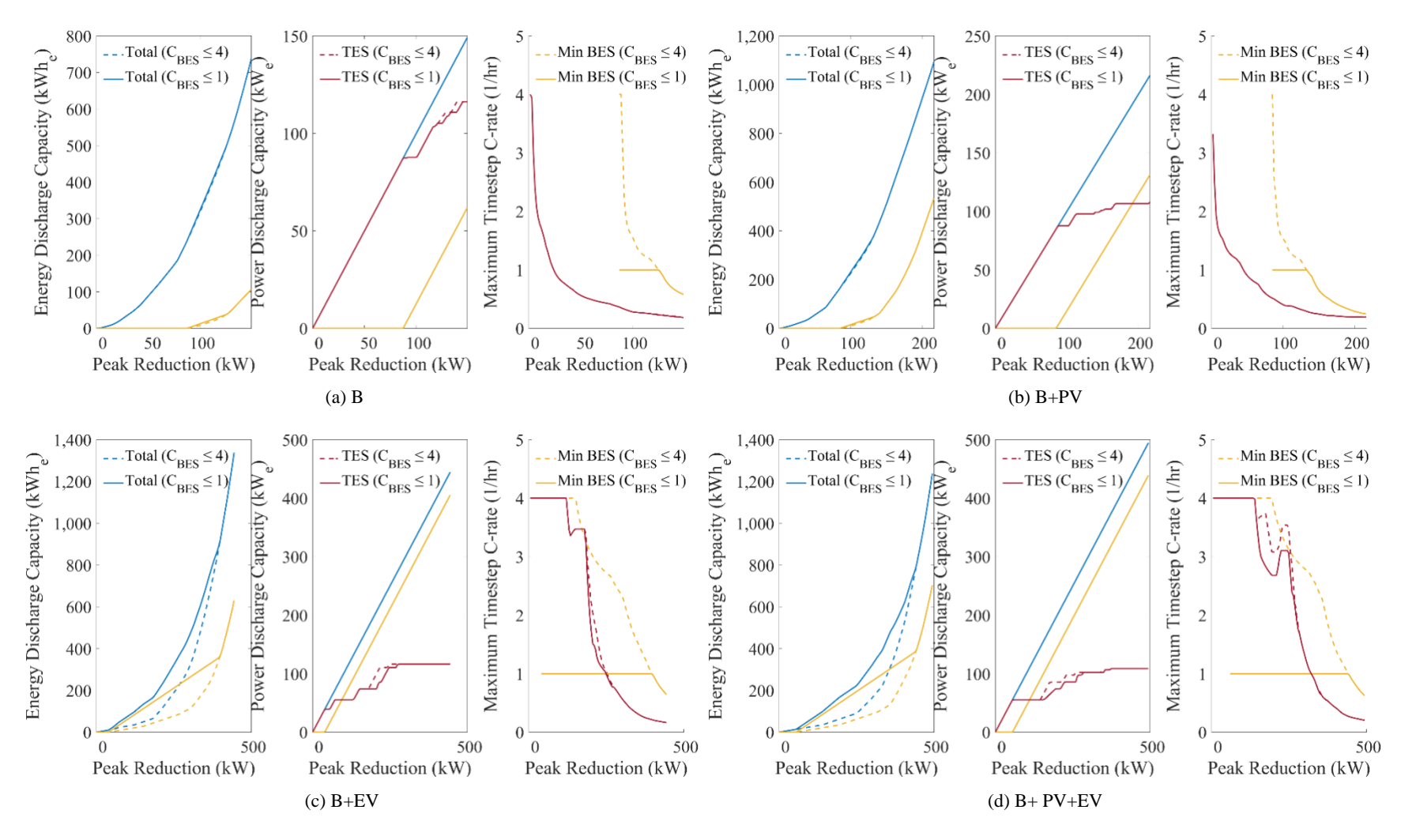


Figure B.2: Impact of peak reduction on required hybrid energy storage capacity (including minimum battery size needed to meet nonthermal loads), required power for both hybrid components, and C-rate for both hybrid components for the four analyzed scenarios: (a) Building only, (b) Building with PV, (c) Building with EV, and (d) Building with PV and EV; Winter design month

Figures B.3 and B.4 show hourly data for July for the baseline Building and B+PV+EV scenarios, respectively. The blue curve is the building without energy storage (Total), while the purple curve is the electric load due to air conditioning (Thermal). Our algorithm first determines how to discharge and charge the thermal storage to reduce the peak as much as possible. When the green dashed line (Thermal with TES) is above the Thermal base line, the thermal storage is being charged, and when it is below the Thermal baseline, the thermal storage is being discharged. This drops the total electric load profile to the red line (Total with TES). This is a "logical" profile showing the contribution from TES when presuming BES is also present and is not necessarily the objective profile for a TES-only system. In the baseline Building-only scenario, the thermal storage is charged at night and discharged during the day. This is typical of current installations of chiller-integrated thermal storage systems, including chilled-water tanks and ice storage systems.

Figure B.4 has four graphs each showing (a) the maximum electrical energy displaced by thermal storage, (b) the maximum electrical energy displaced by battery storage, (c) the maximum power required by TES, and (d) the maximum power required by the battery. In these cases, the day that dictates the size for power and energy is different, and the right two plots are added because this scenario requires a battery for this level of demand reduction.

The plots in Figure B.4 show that the thermal storage requirements are much different when adding PV and EV charging. The PV shifts the charging period to the middle of the day, and the EV charging requires the thermal storage to continually change its charge and discharge power, and in some cases alternate between charging and discharging over a short period.

As the peak reduction is increased for the B+PV+EV scenario, the green dashed line eventually hits zero (at hour 19), and there is no more thermal load to displace at that timestep. This is caused by the spikes due to EV charging. At these points, thermal storage is unable to independently reduce the peak, and a small battery is required to shave the total load to the desired level. The final load profile is the yellow dashed/dotted line, which is the total electric load at the meter when using thermal and battery storage (Total with TES+BES). The difference between the red and dashed/dotted yellow lines is the battery discharge power at that timestep.

In Figure B.4(b), the load is flattened (i.e., all peaks shaved and all valleys filled), meaning the flattened value on July 22 corresponds to the minimum possible peak for this month. Therefore, the storage dispatch strategy must exactly follow the profile shown to obtain the maximum

theoretical peak shaving. Although the peak BES energy utilization occurs on day 22 (Figure B.4 (b)), the peak power occurs on day 31 (Figure B.4(d)), when the EV charging power is higher but for a shorter duration. Therefore, the C-rate limited power requirement is driven by the 31st day even though the 22nd day, with its two lower-power spikes, use more energy.

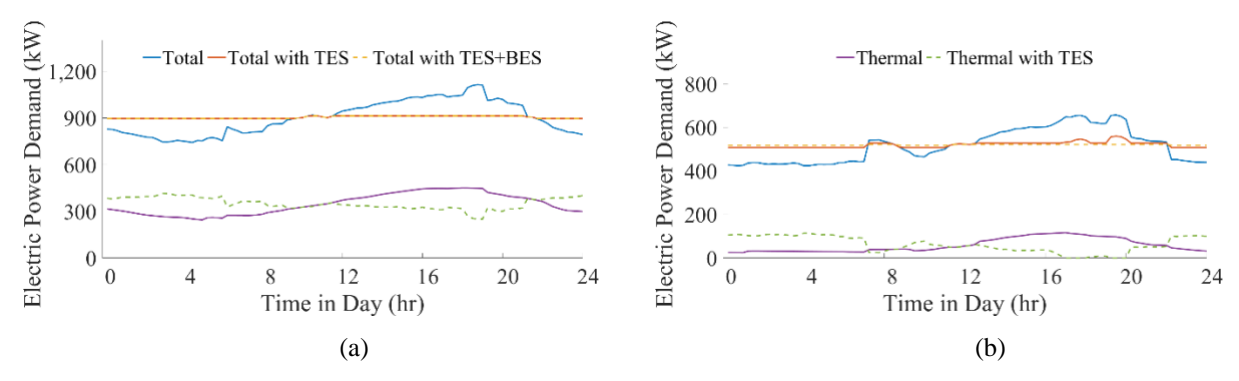


Figure B.3: (a) Daily electric power demand profiles resulting from 200kW shaving in July for the Building scenario; (b) Daily electric power demand profiles resulting from 149-kW shaving in January for the Building scenario.

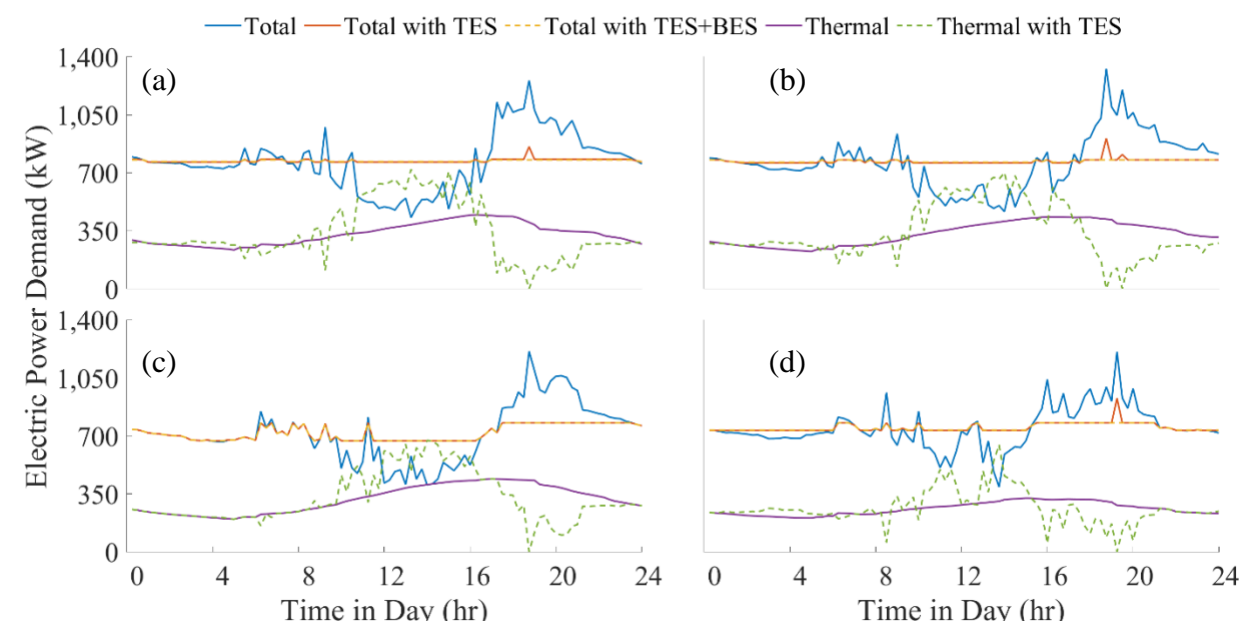


Figure B.4: Daily electric power demand profiles resulting from maximum shaving (549 kW) in July for the B+PV+EV scenario; (a) July 25 showing day with highest TES energy, (b) July 22 showing day with highest BES energy, (c) July 14 showing day with highest TES power, and (d) July 31 showing day with highest BES power